

DEMOCRATIC AND POPULAR REPUBLIC OF ALGERIA  
MINISTRY OF HIGHER EDUCATION AND SCIENTIFIC RESEARCH

**Ecole Nationale Polytechnique**



**Electronic Department**  
**Laboratory of Communication and Photovoltaic Conversion**

In partial fulfillment of the requirement for  
Engineer's Degree

**Design and implementation of a plantar pressure  
measurement system**

Hadjer AZLI

Insaf BOUGUEZINE

**Supervised by:**

PhD. Mourad ADNANE

Prof. Adel BELOUCHERANI

Presented in public on June 21st 2017

**Jury members**

President	Mr. C. LARBES	PhD	ENP
Examiner	Mr. S. BOUKHENOUS	PhD	USTHB
Supervisors	Mr. M. ADNANE	PhD	ENP
	Mr. A. BELOUCHRANI	Professor	ENP

**ENP 2017**



DEMOCRATIC AND POPULAR REPUBLIC OF ALGERIA  
MINISTRY OF HIGHER EDUCATION AND SCIENTIFIC RESEARCH

**Ecole Nationale Polytechnique**



**Electronic Department**  
**Laboratory of Communication and Photovoltaic Conversion**

In partial fulfillment of the requirement for  
Engineer's Degree

**Design and implementation of a plantar pressure  
measurement system**

Hadjer AZLI

Insaf BOUGUEZINE

**Supervised by:**

PhD. Mourad ADNANE

Prof. Adel BELOUCHERANI

Presented in public on June 21st 2017

**Jury members**

President	Mr. C. LARBES	PhD	ENP
Examiner	Mr. S. BOUKHENOUS	PhD	USTHB
Supervisors	Mr. M. ADNANE	PhD	ENP
	Mr. A. BELOUCHRANI	Professor	ENP

**ENP 2017**

# Dedication

*To **my father**, who taught me that the best kind of knowledge is that which is learned for its own sake;*

*To **my mother**, who has always been there for me, doing best what a mother could have ever done;*

*To **my brother and sister**;*

*To my friends for being the most loving, inspiring and supportive friends one could ever ask for. **Mei, Safa, Houda and Madjid**, I would not have made it without you guys.*

*And finally to **YOU!***

*Insaf*

# Dedication

I dedicate this work to the the one who waited patiently for the fruits of her good education, her encouragement, the sacrifices she made to see me succeed *My great mother.*

To the memory of my father who has always pushed and motivated me in my studies, i hope that he appreciates this humble gesture as a proof of gratitude ,may God, the all-powerful, have Him in his holy mercy.

To my brother **Bilel** and my two lovely sisters **Asma** and **Bouchra**.

To my friends,MY BEST friends Karima , Nada and Insaf.

Hadjer

# Acknowledgment

First and foremost, we would like to thank **God** almighty for giving us the strength, knowledge, ability and opportunity to undertake this project and to persevere and complete it satisfactorily. Without his blessings, this achievement would not have been possible.

A special gratitude we give to our supervisors, **Mr.ADNANE** and **Mr.BELOUCHERANI**, whose encouragement helped us take this first step of a long journey.

We would also like to express our deepest appreciation to all those who provided us the possibility to complete this project, especially **Mr.GOMEZ** for his genuine, generous and inspirational support.

We would like to thank our friends for their unconditional love, loyalty and support throughout this entire journey and up to this moment. We cannot cite your names here but you are on our minds.

Last but not least, we would like to thank those whom we can never thank enough. Our parents. We are so much of what we learned from you and for that we are eternally grateful.

## ملخص :

الهدف من هذا المشروع هو تصميم وبناء نظام لاستشعار الضغط الأخمصي. يتكون هذا الجهاز أساسا من أرضية ذات تصميم مستوحى من نموذج مصفوفة استشعار الضغط المرتكزة على تكنولوجيا المقاومة الحساسة للضغط. يتميز الجهاز بأبعاد تقدر ب 1.7سم على 1.4سم للخلية الواحدة.

يتم الحصول على البيانات باستخدام لوحة NI USB 6002 . يتم أيضا اعداد تطبيق باستخدام LabVIEW 14.0 من أجل معالجة البيانات التي تم جمعها وعرض نتائج التحليل. ويشمل هذا الأخير نوعين من أنظمة العرض تصوير أخمصي ثنائي في الوقت الحقيقي وعرض مستوى الرمادي للضغط أخمصي في كل وحدة الاستشعار من المنصة. هذه الواجهة يمكن استخدامها من قبل المعالج لاستخراج بعض المعلومات المكانية وتحديد تشوهات المشية.

**الكلمات الدالة:** تحليل نظام المشيد، أنظمة بلاتار، أجهزة استشعار غير قابلة للارتداء، تكنولوجيا بيزوريسستيف، منصات ضغط

## Résumé:

Le but de cette thèse est de concevoir et construire un system sensitif to pression plantaire qui consiste principalement en un tapis basé sur une technologie piézorésistive. Le design est inspiré par un modèle de détecteurs de pression matriciels et offre une résolution spatiale de 1.7cmx1.4cm

Les données sont acquises au moyen d'une carte NI USB-6002. Une application est implémenté en utilisant NI LabVIEW 14.0 qui a pour but de traiter les donnée et visualiser les résultats de l'analyse de marche sous forme de deux type d'interfaces. Pour la première l'affichage est binaire (noir et blanc) et sert à détecter et tracer les emplacements des pieds du sujet. La deuxième affiche la pression au niveau de chaque élément sensitif du tapis.

**Mots clé :** Analyse de marche, systèmes sensitif de pression, les capteurs résistifs de pression.

## Abstract:

The aim of this thesis is to design and build a plantar pressure sensing system which consists mainly of a piezoresistive technology based mat. The design is inspired by a pressure sensing matrix model and presents a maximum attainable spatial resolution of 1.7cmx1.4cm.

Data is acquired using an NI USB-6002 board .An application is implemented using NI LabVIEW 14.0 in order to process the collected data and visualize the output of the system. This latter includes two types of plantar profile pressure images : A binary-level real time display of the subject's footprint and a grey-level display of the plantar pressure at each sensing unit of the platform.

This interface can be used by a therapist to extract some spatial parameters and determine gait abnormalities.

**Key words:** gait analysis, plantar systems, non-wearable sensors, piezoresistive technology, pressure platforms

# Contents

List of Figures

List of Tables

<b>Introduction</b>	<b>11</b>
<b>1 Gait Analysis</b>	<b>13</b>
1.1 Gait analysis as a diagnosis tool . . . . .	13
1.1.1 Introduction . . . . .	13
1.1.2 Parameters of interest for the human gait . . . . .	13
1.1.3 Basics related to gait analysis . . . . .	15
1.1.4 Gait analysis in clinical applications . . . . .	17
1.2 Gait analysis methods . . . . .	18
1.2.1 Wearable sensors-Based systems (WS systems) . . . . .	19
1.2.2 Non-wearable sensors - based systems . . . . .	21
1.3 Primitive approach to our solution . . . . .	25
<b>2 Force/Pressure Measurement Techniques</b>	<b>28</b>
2.1 Force/Pressure sensors . . . . .	28
2.1.1 Resistive transducer . . . . .	28
2.1.2 Piezoelectric sensors . . . . .	35
2.1.3 Capacitive sensors . . . . .	36
2.1.4 Optical technologies . . . . .	37
2.2 Comparison and technology selection . . . . .	38
2.3 Calibration . . . . .	40
2.3.1 Dynamic calibration methods . . . . .	41
<b>3 Conception and Engineering</b>	<b>44</b>
3.1 Basic structure . . . . .	44
3.2 General description of the mat . . . . .	44
3.3 How does it all work? . . . . .	46
3.3.1 General Mechanism . . . . .	46
3.3.2 Row Selection . . . . .	47
3.3.3 Column selection . . . . .	49
3.3.4 Buffers . . . . .	52
3.3.5 Determining FSRs from the same Row . . . . .	53
3.3.6 Data acquisition . . . . .	54
3.3.7 General structure . . . . .	54
3.3.8 Software Application . . . . .	55



3.3.9	Arduino uno VS. NI USB-6002 . . . . .	55
<b>4</b>	<b>Implementation, Calibration and Final Tests</b>	<b>64</b>
4.1	Calibration . . . . .	64
4.1.1	What makes a good sensor . . . . .	64
4.1.2	Calibration technique . . . . .	65
4.2	Implementation . . . . .	67
4.2.1	The pressure mat . . . . .	67
4.2.2	Conditioning circuitry . . . . .	69
4.3	Software application . . . . .	71
4.3.1	General description of the interface . . . . .	71
4.3.2	Block diagram . . . . .	71
4.4	Final Tests . . . . .	75
	<b>General Conclusion</b>	<b>77</b>
	<b>Bibliography</b>	<b>78</b>
	<b>A AppendixA</b>	<b>81</b>
	<b>B AppendixB</b>	<b>82</b>
	<b>C AppendixC</b>	<b>84</b>
	<b>D AppendixD</b>	<b>85</b>
D.1	NI-USB 6002 . . . . .	85
D.2	Arduino Uno . . . . .	87
D.3	Multiplexer . . . . .	88
D.4	Shift Register . . . . .	89
D.5	Operational Amplifier LM324 . . . . .	89

# List of Figures

- 1.1 Gait cycle analysis . . . . . 15
- 1.2 Diagram summarizing gaiting tools repartitions . . . . . 19
- 1.3 Instrumented footwear for gait monitoring presented by [15] . . . . . 20
- 1.4 working principal of a TOF system . . . . . 22
- 1.5 Structure of a force plate [[19]] . . . . . 23
- 1.6 A schematic representation of one large and two small sensors positioned in close approximation to a localized peak pressure (M is the position of maximum pressure). . . . . 25
  
- 2.1 Bonded strain gauge . . . . . 29
- 2.2 a.Wheatstone bridge circuit; b.Dummy gauge . . . . . 29
- 2.3 PushPull configuration . . . . . 30
- 2.4 ShuntMode and ThruMode sensors . . . . . 31
- 2.5 FSR layers in ShuntMode . . . . . 32
- 2.6 FSR layers in ThruMode . . . . . 32
- 2.7 ShuntMode Matrix layers . . . . . 33
- 2.8 ThruMode Matrix layers . . . . . 34
- 2.9 FSR ink particles when compressed . . . . . 34
- 2.10 converse and direct effect . . . . . 36
- 2.11 capacitive sensor with waveform profile . . . . . 37
- 2.12 A Fiber Bragg Grating structure, with refractive index profile . . . . . 38
- 2.13 spectrum response of FBG . . . . . 38
- 2.14 structure of a floor using FSR [36] . . . . . 39
- 2.15 Dynamic calibration with periodic shaker . . . . . 41
- 2.16 Step Force Calibration . . . . . 41
  
- 3.1 Block diagram . . . . . 44
- 3.2 Side view of the pressure mat . . . . . 45
- 3.3 4" x 6" Sensor Fil Kit . . . . . 45
- 3.4 top view . . . . . 46
- 3.5 Functioning Principal . . . . . 47
- 3.6 Row Read . . . . . 48
- 3.7 Column selection using 4067 Demultiplexer . . . . . 49
- 3.8 Ghosting . . . . . 49
- 3.9 Illustration of the data interdependence in a mux-based activation case . . 50
- 3.10 illustrated Solution for data inter-dependence . . . . . 51
- 3.11 Ghosting elimination . . . . . 51
- 3.12 Simulation with no buffers . . . . . 52
- 3.13 Simulation with buffers . . . . . 53

3.14	Matlab Packages for Arduino . . . . .	55
3.15	labview creating project . . . . .	56
3.16	Technical specification of the Arduino UNO R3 board [42] . . . . .	56
3.17	technical specification of NI USB-6002 (datasheet) . . . . .	57
3.18	NI-USB 6002 Pin guide [43] . . . . .	57
3.19	basic circuit for accuracy tests . . . . .	58
3.20	Reading analog voltage -arduino code . . . . .	58
3.21	Reading analog voltage-arduino IDE . . . . .	59
3.22	Analog read with External Aref . . . . .	59
3.23	reading with External Aref . . . . .	60
3.24	FSR element test . . . . .	60
3.25	Sample and hold-arduino board . . . . .	61
3.26	Analog read using buffers . . . . .	61
4.1	Calibration of FSR . . . . .	65
4.2	testing circuitry . . . . .	65
4.3	table of calibrated FSR . . . . .	66
4.4	calibration of the force sensor by the fabricator . . . . .	67
4.5	(a)Mat construction . . . . .	68
4.6	(b)Mat construction . . . . .	68
4.7	Final Result . . . . .	69
4.8	Schematic capture . . . . .	69
4.9	Design Rule Manager . . . . .	70
4.10	Printed circuit with two side . . . . .	70
4.11	Printed circuit with two side . . . . .	71
4.12	LabView Block diagram . . . . .	72
4.13	Block 1 . . . . .	72
4.14	Block 2 . . . . .	73
4.15	Block 3 . . . . .	74
4.16	Matlab SubVi . . . . .	75
4.17	code MatLab . . . . .	75
B.1	Mechanical properties of UHMWPE . . . . .	83

# List of Tables

1.1	Overview of gait parameters [1] . . . . .	14
1.2	Summarized result of frequency/velocity study on 800 people . . . . .	16
2.1	Comparison of different strain gauge Wheatstone bridge configuration . . .	31
4.1	NI 6002 pin redirection . . . . .	73

# Introduction

Gait analysis is nowadays a domain that stands out for its application as a reliable tool for both clinical diagnosis and classification thanks to the amount of effective research dedicated to it.

Long gone are the days in which physical therapists and clinicians relied entirely on observation and common sense. Over the past three decades, equipment and methodology used for gait analysis has progressed considerably. Traditional subjective methods became outdated methods of treatment and have been replaced with state-of-the-art technology that is changing lives of accident victims, injured athletes, and those with central nervous and musculoskeletal systems.

Furthermore, these systems allow us to use gait as a biometric measure to recognize known persons and classify unknown subjects.

We are particularly interested in pressure platforms. We believe that they are to become more and more accessible as a lot of effective research have been and continue to be done as to develop cheaper, more practical and more accurate systems. These systems are also interesting since they are totally unobtrusive which makes it possible to assess gait in its most natural form. They also allow clinicians to keep an eye on their patients while they go about their daily lives. Consequently, they can be used to predict fall which is of a crucial importance for elderly patients who live alone, to identify those who run a higher risk of death and severe morbidity following heart surgery or for many other utilities.

Our project is to design and build a plantar pressure sensing system that is mainly dedicated to medical applications. The system is to be eventually used for implementation of extra data/signal processing algorithms. However, this work -acheived within a restricted time frame- focuses on the design of the hardware of the system including the pressure sensing mechanism itself which is then illustrated by a simple software application.

This report describes the different steps of the process which relies mainly on a top down method. The first chapter gives an introduction to gait analysis as to know what is expected from our system. The second chapter discusses the different technologies that can be adopted and ends with a justified selection and a brief description of the calibration of such systems. The third chapter explains the mechanism of the system and summarizes the design process with different problems and solutions. Last but not least, the fourth chapter describes the implementation of each part of the system and is followed by a report of some tests and a general conclusion.

# CHAPTER 1

# Chapter 1

## Gait Analysis

This chapter is to give a clearer idea of gait analysis, its applications as well as tools used in this domain. It also elaborates some basics concerning human gait in both its normal and abnormal forms.

### 1.1 Gait analysis as a diagnosis tool

#### 1.1.1 Introduction

Gait analysis is the systematic measurement, description and evaluation of a subject's walking pattern using the eye and the brain of observers, enhanced by different instrumental technologies which include kinematics, kinetics, electromyography, video recordings and energy expenditure.

It is commonly used for clinical applications, and that is to assess, plan, and treat or rehabilitate individuals with pathological conditions affecting their ability to walk or even for evaluating the effectiveness of prosthetic limbs. Another application that seems to have drawn some attention lately is gait recognition and classification for security purposes.

#### 1.1.2 Parameters of interest for the human gait

Specialists evaluate patients gait by using various methods that measure parameters which most clearly represent the human gait. The factors of interest in a such research may vary depending on the field of this research.

In sports field for instance, research may center on the analysis of the different forces exerted on each muscle. If we center on the clinical point of view, gait velocity for example is a simple effective test that can identify subgroups of elderly patients who run a higher risk of death and severe morbidity following heart surgery.

Table 1.1 indicates a list of parameters that are interesting for each research field.

- Short step length is the distance between two successive placements of the same foot.
- The stride length is the distance between the placements of both feet
- Cadence or rhythm is the number of steps per time unit. In normal gait, cadence is about 100-115 steps per minute.
- Step width is the linear distance between two equivalent points of both feet.

Gait parameters	Application		
	Clinical	Sports	Recognition
Stride velocity	X	X	X
Step length	X	X	X
Stride length	X	X	X
Cadence	X	X	X
Step width	X	X	X
step angle	X	X	X
Step time	X		
Stance time	X		
Swing time	X		
Traversed distance	X	X	
Gait autonomy	X		
Stop duration	X		
Existence of tremors	X		
Fail	X		
Accumulated attitude	X	X	
Route	X	X	
Gait phases	X	X	X
Body segment orientation	X	X	
Ground reaction forces	X	X	
Joint Angles	X	X	
Muscle forces	X	X	
Momententum	X	X	
Body posture (inclination, symetry)	X	X	X
Long term monitoring of gait	X	X	

Table 1.1: Overview of gait parameters [1]

- Step angle is the direction of the foot during the step.
- Short step time the duration from placement of a foot to the next placement.
- Swing time for each foot is the time from the moment the foot lifts from the floor until it touches it again, for each foot.
- Support time or stance time is the time from the moment the heel touches the floor until the toes are lifted, for each foot
- Gait autonomy is the maximum time a person can walk, taking into account the number and duration of the stops
- Duration of the stops the time during which the subjects is not walking.
- Tremors: Involves the assessment of the steadiness of foot when taking a step.
- Accumulated attitudes: Uneven terrain covered (height difference between drops and rises). The quality of the taken route is to be considered as well.
- Joint angles correspond to the direction of leg segments and include the angles of different joints (ankle, knee, hip)



- Ground Reaction Forces : is the force exerted by the ground on a body in contact with it.
- Electrical activity produced by muscles (EMG) : An electromyograph detects the electric potential generated by muscle cells, when these cells are electrically or neurologically activated.
- Body posture which includes bending and symmetry[1]

In the following sections we see how these parameters can be linked to a variety of physical alterations. We also take a closer look at some generalities and basic notions of gait analysis as to define the aim of this project.

### 1.1.3 Basics related to gait analysis

#### Gait cycle (GC)

One important aspect to learn about when dealing with gait analysis is the gait cycle. Gait cycle is also known as a full step: It starts with a particular foot placement and ends with the next placement of the same foot. It mainly consists of two phases, each with numerous sub-phases. This partition may be more or less accurate depending once again, on the field of research. Figure 1.1 illustrates the most important sub-phases of the human gait. It is the task of this project to visualize each of these sub-phases.

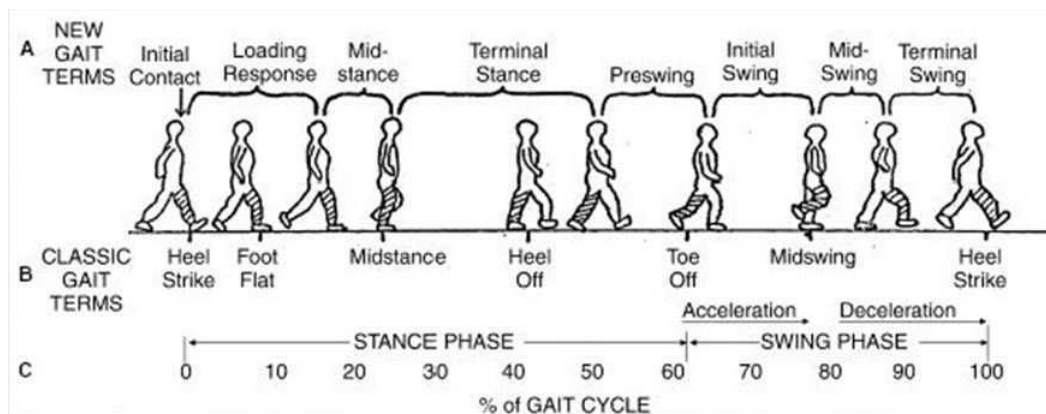


Figure 1.1: Gait cycle analysis

When analyzing gait cycle one foot is taken as reference and the movements of the reference foot are studied. A gait cycle can be divided as follows:

1. Stance Phase: The stance phase is that part of a gait cycle during which the foot is in contact with the ground. It constitutes of 60 % the gait cycle it mainly comprises:
  - Initial Contact (Heel Strike) 0%:Occurs when the heel of the reference foot first touches the ground. This sub-phase is almost instantaneous.
  - Loading Response (Foot Flat)0-12% :Marks the beginning of the initial double limb stance. The weight is transferred onto the referenced leg. This sub-phase is important for weight-bearing, shock-absorption and forward progression of the body. Hence, the loading response period probably is best described by the typical quantified values of the vertical force curve. Matter of fact, the

ascending initial peak of the vertical force graph reveals the period of loading response.

- Mid Stance 12-31 % :From elevation of opposite foot until both ankles are aligned in the coronal plane. It involves alignment and balancing of body weight on the reference foot.
- Terminal Stance 31-50%: begins when the supporting heel rises from the ground and continues until the opposite heel touches the ground. In this phase the heel of reference foot rises while its toes are still in contact with the ground. The ascending second peak of the vertical force graph demonstrates the period of terminal stance.
- Toe Off (Pre Swing)50-60%: from initial contact of opposite limb to just prior to elevation of ipsilateral limb. In this phase, the toe of the reference foot rises and swings in air. This is the beginning of the swing phase of the gait cycle.

2. Swing Phase: The swing phase is that part of the gait cycle during which the reference foot is not in contact with the ground and swings in the air. It constitutes about 40% of gait cycle. It has three parts:

- Swing (toe off): From elevation of reference limb to the point of maximal knee reflection. It is characterized by initial acceleration of the reference foot.
- Mid Swing: Reference foot is suspended in the air almost horizontally.
- Terminal Swing: It's characterized by a general deceleration of the reference foot. Locked extension of the knee and a neutral position of the ankle are observed.

The terminal swing phase occurs at the same time as the loading response phase of the opposite foot [2, 3, 4].

**Frequency and velocity of people walking:**

Walking frequency and velocity of individuals may vary according to gender, age, fitness, temperature, weather ,etc. the table 1.2 below presents the average frequency and velocity range on footbridges and shopping floors collected from a study on 800 people.[5]

	Footbridges	Shopping floors
Frequency range	1.4Hz - 2.1Hz	1.7Hz - 2.5 Hz
Velocity range	0.93 - 1.8 m/s	0.99 - 1.8 m/s
Mean value of step length	0.71 m	0.71m
Mean value of walking frequency	1.8Hz	2.0Hz
Mean value of walking velocity	1.3m/s	1.4m/s

Table 1.2: Summarized result of frequency/velocity study on 800 people

The mean values of the step-length on the footbridges and the shopping floors are similar with 0.75m for men and 0.67m for women. These studies combined with the gait cycle analysis, are important when it comes to estimating the requirement performances of a gait analysis system.

## 1.1.4 Gait analysis in clinical applications

### 1.1.4.1 Introduction

If we center on the clinical point of view which is the primal target of our project, countless of applications have been brought to action in the last few decades whether they are meant for testing (diagnosis) or research usage. The importance of human gait analysis lies in the fact that gait abnormalities are key signs of many disorders. On one hand, this makes early diagnosis of diseases and their complications possible by collecting accurate information on the patient's gait at a given moment, and/or over a period of time and comparing them to healthy gait patterns. On the other hand, It also helps assess the state of those with gait pathologies related diseases in order not only to determine the severity of the disease or injury, select a treatment and predict prognosis, but also for better understanding of the disease. For instance, velocity can help identify subgroups of elderly patients who run a higher risk of death following a heart surgery [6] . Moreover, Gait analysis is the key tool when it comes to many rehabilitation procedures following strokes and/or injuries. Significant kinematic deviations observed in swing phase for example include decreased peak hip flexion, decreased peak knee flexion, decreased knee extension for heel strike and decreased ankle dorsiflexion throughout swing [7].

Gait analysis is also used for orthopedic plantation assessment. It can be used in fall prevention, particularly with elderly people, it is even recommended for merely enhancing the gait quality of the subject as to prevent potential pathologies. Some of the gaiting techniques can be remote. This maximizes an individual's independence and help solve bigger scale problems like health-care requirements overflow, especially in case where people don't always have access to this kind of health-care.

### 1.1.4.2 Gait related pathologies

This section could be detailed into a sequel of great interest to a specialist in the medical field. However, our study focuses on the electronics engineering part so we will settle for a few examples of gait abnormalities with some of their respective gait patterns characteristics.

#### **Abnormalities :**

- **Antalgic Gait:** This kind of gait develops as a way to avoid pain while walking. Pain is generally caused by muscular rupture or tear. It is characterized by a shortening of the stance phase on the affected side which corresponds to an increase in stance phase on the unaffected side.
- **Functional Leg-Length Discrepancy:** it is when the paired lower limbs have unequal length. This manifests through a number of compensations such as circumduction, hip hiking, step-page, etc. This kind of gait is also characterized by a swing phase longer than the stance phase for the affected foot, weak hip flexing, etc . [8]
- **Inadequate Dorsiflexion Control:** Characterized by a foot slap in stance phase and toe-dragging in swing phase. This is usually caused by what specialists call spastic plantar-flexors which is a condition in which certain muscles are continuously contracted. This contraction causes stiffness or tightness of the muscles and can interfere with normal movement, speed, and gait.[9]

- **Excessive Knee Extension:** Loss of the normal knee flexion during stance phase. The knee may go into *hyperextension* or *Geni recuatum* [10] which is an abnormality that causes the knee to bend backward when the person is in a standing position.
- **Parkinsonian gait:** The patient generally has rigidity, *bradykinesia* - slow movement often associated with an impaired ability to adjust the body's position- and tremor. He or she will be stooped with the head and neck forward, with flexion at the knees and walk with slow little step.  
This kind of gait is also characterized by a difficulty in initiating steps, and the patient may show an involuntary inclination to take accelerating steps, known as festination. This gait is seen in Parkinson's disease or any other condition causing parkinsonism, such as side effects from drugs.
- **Ataxic gait:** Most commonly caused by damage to a part of the brain known as the cerebellum or by damage to the spinal cord or other nerves, this gait is described as uncoordinated, staggering movements with a wide-based gait.  
While standing still, the patient's body may titubate -swagger back and forth-, walking is characterized by a inability to remain within a straight line. Acute alcohol intoxication's gait is very similar to ataxia. Patients with more truncal instability are more likely to have midline cerebellar disease at the vermis -an area in the brain- [11]

## 1.2 Gait analysis methods

**Semi-subjective vs. Objective methods:** Traditional methods consist of making the patient walk and observing the quality of their gait then -in most cases- asking the patients to give a subjective evaluation of the quality of their own gait. These methods are thereby not dependable as they rely utterly on human eyes alone. Their measurements lack accuracy and precision, and can only be considered as primitive. An example of this kind of gait analysis procedure is elaborated in [7] .

Progress in new technologies has led the development of a series of devices and techniques which allow for a much more objective evaluation, (Although the degree of objectivity varies from one technique to another) making measurements more efficient and providing specialists with more reliable information. Objective gait analysis techniques are based on the use of different devices to capture and measure information related to the various gait parameters.

On the whole, it can be seen that three different approaches are deployed: image processing, floor sensors and sensor that are placed on the body. These technologies can be classified into one of the following categories see Figure 1.2 .

- *Those based on wearable sensors (WS):* they use sensors placed on different parts of the body, such as feet, knees or thighs
- *Those based on non-wearable sensors (NWS):* which can be classified into two sub-groups:
  - image processing (IP).
  - floor sensors.

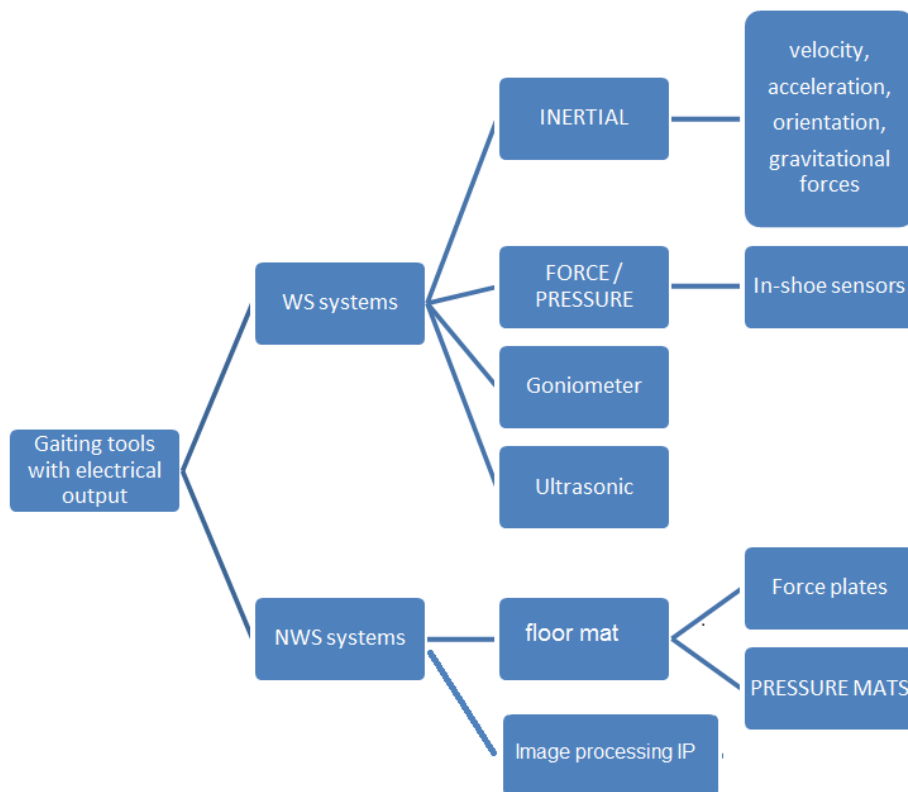


Figure 1.2: Diagram summarizing gaiting tools repartitions

### 1.2.1 Wearable sensors-Based systems (WS systems)

As their name indicates, these systems are placed on various parts of the patient's body, such as feet, knees or hips to measure different characteristics of the human gait. What is interesting about wearable systems is that they are totally non-obtrusive devices that allow clinicians to "remotely" monitor individuals over extended periods of time. This is prominent in cases with chronic diseases conditions [12]. Physicians want to monitor individuals whose chronic condition includes risks of sudden acute events or individuals for whom interventions need to be assessed in the home and outdoor environment. If observations over one or two days are satisfactory, ambulatory systems can be utilized to gather physiological data. An obvious example is the use of ambulatory systems for ECG monitoring, which has been part of the routine evaluation of cardiovascular patients for almost three decades. [1] Wearable sensors include force sensors, accelerometers, gyroscopes, extensometers, inclinometers, goniometers, active markers, electromyography, etc.[13]

#### 1.2.1.1 Pressure and force sensors

They come in in-shoe pressure and force sensing systems. These systems are based on pressure / force sensing transducers such as piezoresistive elements, piezo electric elements, capacitive elements and so forth. They measure the Ground Reaction Force ( $GRF$ ) under the foot and return a current or voltage proportional (desirably) to the pressure measured. The main difficulties with this type of measurement are the curvature that characterizes the surface ( the sole of the shoe) Figure 1.3, the lack of space for the transducers and

the need to run large numbers of wires. However, miniaturized sensors technology have known a remarkable growth given the rapid technological advances in health-care monitoring equipment, micro-fabrication processes and wireless communication. A number of commercial systems are therefore now more and more available. These sensors are widely used in instrumented shoes such as those developed in [14]

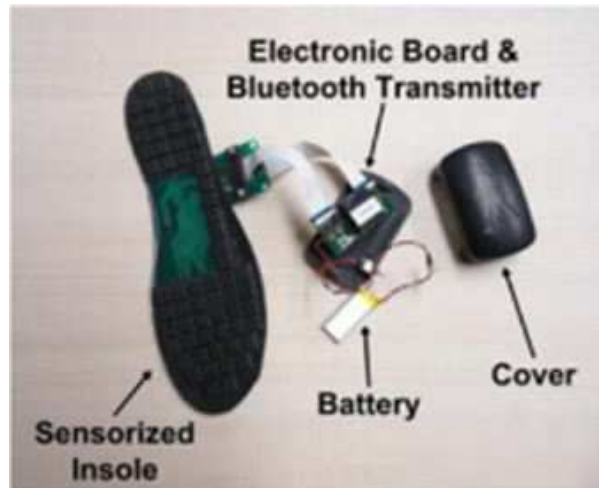


Figure 1.3: Instrumented footwear for gait monitoring presented by [15]

### 1.2.1.2 Inertial sensors

Inertial sensors are electronic devices that measure and report an object's velocity, acceleration, orientation and gravitational forces, using a combination of accelerometers, gyro sensors and sometimes magnetometers. Inertial sensors can be built in miniature sizes which permits integrating them into instrumented insoles for gait analysis. Such systems also include Bluetooth communication modules, Charging systems, etc... [1]

**Accelerometers** : An accelerometer is an electromechanical device that measures acceleration forces. These forces may be static, like the constant force of gravity, or they may be dynamic-caused by moving or vibrating the accelerometer.

#### **How an accelerometer works** :

It's a combination of 3 force capacitive MEMS (micro electro-mechanical) sensors placed along the 3 axis(x,y,z), with capacitance that changes with the the amount of force applied along a given axe : A silicon weight is attached to one of its terminals causing the capacitance to change as the applied GRF moves it back and forth. [16]

**Gyrosensors** :Gyro sensors, also known as angular rate sensors or angular velocity sensors, are devices that sense angular velocity from the Coriolis force applied to a vibrating element. consequently, the accuracy with which angular velocity is measured differs significantly depending on element material and structural differences.

### 1.2.1.3 Ultrasonic sensors

Ultrasonic sensors are used for distance measurements between the two feet as to measure and draw the trajectory of one foot in respect to the opposite foot during gait. An emitter and a receiver of ultrasonic waves are placed on the reference foot. Distance is measured based on the time lapse that the wave takes to travel from and back to the same foot. A more elaborate application of ultrasonic sensors in gait analysis can be found in [17]

### 1.2.1.4 goniometers

A goniometer is an instrument used to measure angles. In gait analysis, we typically use strain gauge-based goniometers which possess on a resistance value that changes according to how flexed the sensor is. These sensors can be used to study the angles for ankles, knees, hips, etc. When a joint is bent, the sensor attached to it is flexed. Consequently, the material forming it stretches, which means the current going through it has to travel a longer path which is translated to an increase in the sensor's resistance.

## 1.2.2 Non-wearable sensors - based systems

### 1.2.2.1 Image processing IP

An IP system relies mainly on an analog or a digital camera with lenses that is used to collect gait-related information. Several techniques are applied such as "threshold filtering" which converts images into black and white. This technique is followed by the "pixel count" to count the number of light or dark pixels and/or the background segmentation to simply omit the background of the image [1]. IP gait analysis methods consist of a collection of techniques which are used to calculate and obtain a map of distances from a viewpoint and it can even reconstruct a 3D modeling of the assessment environment. These techniques make it possible to obtain important elements of the image with a better and faster real-time process. They basically fall into what we call depth measurement technology from which 4 IP methods are derived:

**Camera triangulation (Stereoscopic vision)** : This method is inspired by the human ability to determine the depth of a particular point or object along with the length and the width of any object placed before the eyes and that is based on two slightly different captures of the same scene by each eye. This is simulated through a stereo camera system. The process begins with identifying image pixels that correspond to the same point in a physical scene, The 3D position of a point can then be established by triangulation i.e. calculation of similar triangles between the optical sensor, the light-emitter and the object in the scene. This technique is widely used for gait analysis.[18]

**Time of flight systems -TOF** :A time-of-flight camera (ToF camera) is a range imaging camera system that resolves distance based on the known speed of light.

**Functioning principle** : The observed scene is illuminated with modulated near infrared luminous signal.This signal is modulated with a known frequency. The reflected light is projected onto a detector (complementary metal oxide semi-conductor for example).The shift in phase indicates the covered distance and is measured in parallel with each pixel.Figure 1.4

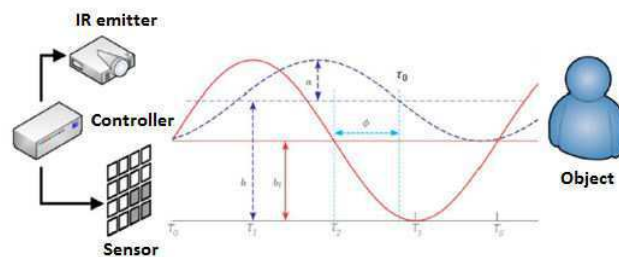


Figure 1.4: working principal of a TOF system

**Structured light** : In this method, a light pattern is projected onto a scene under geometric calibration. Based on how the illumination pattern deforms when striking surfaces, the depth and surface information of the objects in the scene are calculated by vision systems . One of the common devices which use this technology is the Kinetic sensor, which is also used in many gait analysis laboratories.

**Infrared thermography-IRT:** Infrared thermography is the science of detecting infrared energy emitted from an object, converting it to apparent temperature, and displaying the result as an infrared image. it creates visual images based on surface temperatures. As in turned this technology is helpful when it comes to gait analysis.

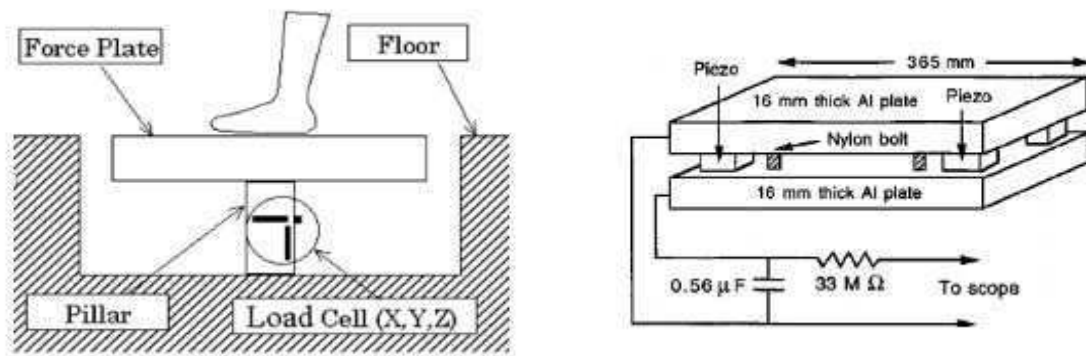
### 1.2.2.2 Floor sensors

Floor sensing systems include force or pressure sensors spread over a given area on the floor, forming in most cases an array of sensing tiles or any other type of sensing elements. Gait is measured through detected force/pressure that is applied by the subject on the sensing elements as he/she walks on the platform. Parameters detectable by such technique include: Cadence, swing phase , stance phase , velocity, center of mass and its displacement, symmetry ratios, etc.(Note that this is exactly the aim of this project). What is interesting about sensing floors is two properties: Low invasiveness and high invisibility i.e, the sensing layer is similar to traditional floor and thereby invisible to the users which allows to avoid the observers effect Research on non-invasive human-computer systems has attracted a wide interest.

Techniques used for plantar measurements are classified due to the diversity of transducers, and the types of the output : Electrical signal is the most desirable form of output since it is readily amenable to processing, storage, analysis and display. However, some techniques produce output either as an immediate hard copy (such as footprinting) or through an optical interface (such as video).

**Force plates** Force plates consist of a top plate (mounted level with the surrounding floor) separated from a bottom frame by the force transducers mounted either near each corner or at the center Figure .1.5 .Any force exerted on the top surface is transmitted through the force transducers. force plates enable one to measure not only the vertical and shear forces but also the center of pressure during gait.





(a) One sensig element mounted at the center (b) Four sensing elements mounted at the corners

Figure 1.5: Structure of a force plate [[19]]

Force plates uses different types of sensing element: piezoelectric strain gauge, capacitive, etc. These elements give an electrical output proportional to the applied force. The electrical signal is then conditioned, processed and visualized by the specialist. A force platform can include one or multiple force plates depending on its application.

Tens of articles have been published since the late 80s regarding applications of force platforms. For instance, the platform at [20], based on strain gauge cells, is used for identifying people based on their footstep with a recognition rate of 93%, while the one at [21] is a square grid of conventional carpet tiles, each backed by plywood and a steel plate, supported at the corners by cylindrical load cells that are instrumented to give us the total vertical force. Rainone, Gardner, and Frost had designed a force plate based on an octagonal strain ring to support the four corners of a rigid top plate. strain gauges were mounted on two sides of each of the four rings at each end of the plate two corresponding rings are mounted perpendicular to each other in order to measure the forward and lateral forces. this design allow the instrument to simultaneously measure forces produced along three different axes, without cross-talk between the respective directions.

Force platforms are also used in biomechanics laboratories to measure ground forces involved in the motion of human or animal subjects. Cross from the university of Sydney leads in a study on human gait in walking, running or jumping and shows that force plates can be used *as excellent teaching aid in a physics class or laboratory, to demonstrate relationships between force, acceleration, velocity, and displacement*. Examples of commercial force platforms:

- Kistler force plates of different types,
- Force platform AMTI series OR6-7 of Biometrics France, etc.

What prioritizes Force Platforms over Pressure Platforms is that force platforms give **absolute** measurements of the three components of a given force. However, the use of FP systems is usually restricted to gait analysis under laboratory environments as installation procedures are laborious and costly [23]. Most force platforms are even mounted onto the floor. Hence, comes the necessity of more flexible systems in terms of commodity and transportability. That is where Pressure Platforms systems come.

**Pressure Platforms** Pressure measurement systems come in high resolution arrays of pressure sensing elements. They are useful for quantifying pressure (vertical) patterns under a foot over time but cannot quantify horizontal or shear components of the applied forces. Pressure is generally given in percentage of weight and that is in regard to comparing the patient's data. Pressure varies during the time the foot is in contact with the floor. The maximum pressure occurs when the heel touches the floor and when the toes push off to take another step. During this time, pressure may reach up to 120%–150% of the patient's body weight according to Muro-de-la-Herran, Garcia-Zapiran, and Mendez-Zorrilla.

At each sampling, The pressure platform is scanned, electrical output for each sensing element is used to calculate the corresponding pressure, a "pressure image" composed of pixels is generated. Each of the pixels on the image corresponds to a sensel such that a sensel is the smallest area defined by one sensing element and across which pressure is supposed to be constant. Pressure applied on top of a sensor is translated to a scaled intensity or colour of the corresponding pixel.

Two types of pressure images can be obtained according to the sensor capabilities in terms of accuracy, hysteresis, and repeatability:

- binary pressure images: generated in case of switch-like sensors i.e. When a switch sensor is pressed, the corresponding pixel value is switched to on. Information drawn from this kind of images are limited and related only to people or object displacements on the pressure platform, which results in the loss of the information related to the subject's weight or the variation of the applied pressure.
- grey-level pressure images: generated by systems based on good-quality continuous sensors. Each pixels value is a function of pressure applied to the corresponding sensors. Grey-level images are characterized by a higher information content.

Consecutive temporal pressure images can be collected as frame sequences to generate a pressure video. This allows to detect and determine spatio-temporal events on sensing floors. [24]

**Sensing technology** Different types of sensors can be used (see chapter 2). the Resolutions which depends majorly on the sensors type is a key parameter when it comes to pressure platforms. Some complex systems have a sensor matrix up to four sensors per  $cm^2$  which makes it possible to measure the differentiated pressure of each zone of the foot separately over time to obtain more significant information. [1]

**The relationship between the pressure and the sensor size** A soft-tissue contact surface will have regions of high and low pressure. Pressure that results from a force  $F$  applied at  $M$  and collected by a small sensor located at  $M$  is more accurate than that collected by a bigger size pressure sensor as this latter will collect the average pressure over its effective area. Hence, The importance of resolution. On the other hand, if the sensing element is too small for a sensel the resulting pressure is also inaccurate (increase in insensitive area). consequently. a single sensor's surface has to be as close as possible to the surface of the sensel.

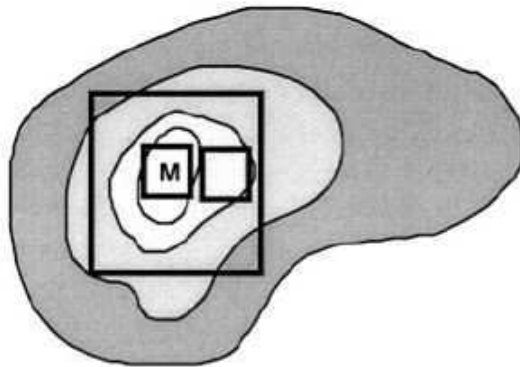


Figure 1.6: A schematic representation of one large and two small sensors positioned in close approximation to a localized peak pressure (M is the position of maximum pressure).

### 1.3 Primitive approach to our solution

The idea is to design and build a non wearable pressure platform designed for medical purposes. A top down method is adopted. Note that the aim of this work is to make a mere proof of concept i.e. a project built to test a concept or process or to act as a thing to be replicated or learned from. Choice of technology deployed in the sensing element depends majorly on accessibility to necessary material and fabrication procedures.

The system aim is to generate a time scale high resolution profile of the patient's feet, from which several gait parameters are drawn including step length, stride length, step time, stride time, swing time, stance time, cadence and symmetry ratios. Measurement are to be visualized on a graphical interface where pressure images are displayed (see previous section).

**Physical properties:** Best spatial resolution possible, best part-to-part repeatability which has to do with the fabrication methodology as well as the homogeneity of the used material.

**Load range:** The prototype has to present a load range that goes up to 225 kg which is 150% of a weight limit of 150kg and that is over an area of approximately 30cm x 10cm which is equivalent to the minimum foot size of an adult subject (we don't need to worry about younger subjects since they can't reach the weight limit).

**Mechanical properties:** Materials used in this project have to present proper functioning within ambient temperature range. They must also ensure repeatability, durability and dynamicity. This latter mainly depends on the elasticity of the material used at any point of the fabrication process.

**Current must be kept low:** Overheating may destroy the device, heat sinks are used when necessary.

**Temporal resolution:** In an ideal case, the scanning frequency is at least 100 times per gait cycle. Temporal resolution = 1% of the gait cycle duration which corresponds to maximum walking frequency. It supposed that the subject's walking frequency on the pressure platform is less than that on foot bridges or shopping floors. and has a maximum value of approximately 1.2 Hz. This results in a minimum scanning frequency of about 120 scans/sec.

## Conclusion

This chapter is to draw the technical specifications of the project and that is in terms of type of the required measurement and temporal and spatial resolution. It also discussed aspects of the human's gait that are to be visualized when the system has been implemented. A brief description of the different technologies used for gait analysis can easily point out the importance of such system.

## CHAPTER 2

# Chapter 2

## Force/Pressure Measurement Techniques

Measurement of the pressure beneath the foot is a specialized form of gait analysis which allows the study of the pressure distribution across the sole, many methods and techniques were developed over time from static to dynamic methods. This chapter points out these different technologies and methods.

### 2.1 Force/Pressure sensors

#### 2.1.1 Resistive transducer

A resistive sensor is a type of transducers that changes its resistance -in most cases- proportionally to an applied amount of force. The most used forms of resistive transducers are strain gauge load cells and force sensing resistors named “FSRs” by *Interlink electronics*. Other types of load cells include hydraulic load cells and pneumatic load cells. FSRs use conductive rubber (elastic), conductive ink or polymers.

##### 2.1.1.1 Strain gauges

A load cell is a transducer that is used to create an electrical signal whose magnitude is directly proportional to the measured force. Strain gauges consist of thin wires. Alternatively, conductors may be thin strips of metallic film deposited on a non-conducting substrate material called the carrier.

Electrical resistance (R) of a metal wire is given by

$$R = \frac{\rho L}{A} \quad (2.1)$$

where  $\rho$  is the resistivity, L and A are respectively the length and the cross section of the wire. This equation shows that the resistance is proportional to the length (L) and inversely proportional to the area (A).

Consequently, if a strip of a conductive metal is placed under a compressive force, it broadens and shortens and its resistance vary. If this stress is kept within the elasticity limits (without deformation), the strip can be used as a measuring element for physical force, the amount of applied force inferred from measuring its resistance. This is used to measure the strain in the structure. Figure 2.1 also shows how strain gauges are generally insensitive to lateral forces.

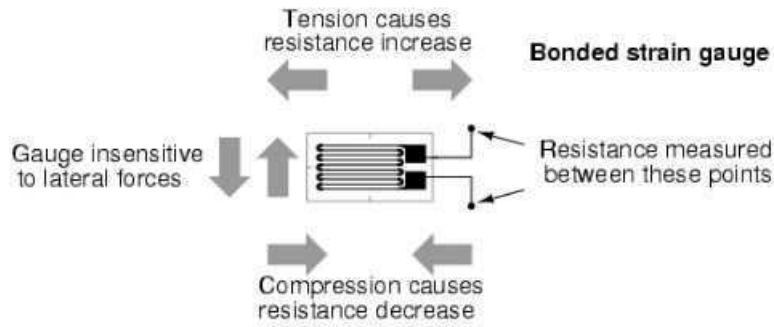


Figure 2.1: Bonded strain gauge

The ratio of the fractional change in electrical resistance to the fractional change in length, or strain is known as the gauge factor(GF). The GF for metallic strain gauges is usually around 2.

**Strain gauges in Wheatstone Bridges:** In practice, strain measurements rarely involve quantities larger than a few millistrain ( $\epsilon \times 10^{-3}$ ). Therefore, to measure the strain, we have to accurately measure very small changes in resistance. This is why strain gauges are connected in Wheatstone bridge circuits which indicate measured strain by the degree of imbalance

The three types of strain gauge configurations, quarter-, half-, and full-bridge, are determined by the number of active elements in the Wheatstone bridge, the orientation of the strain gages, and the type of strain being measured.

For example, the circuit in Figure 2.2a is a half bridge. It allows us to minimize the temperature effect. In practice this can be implemented using a strain gauge configuration where one gauge is active  $R_G + \Delta R$ , and a second gauge is placed transverse to the applied strain as shown in Figure 2.2a.

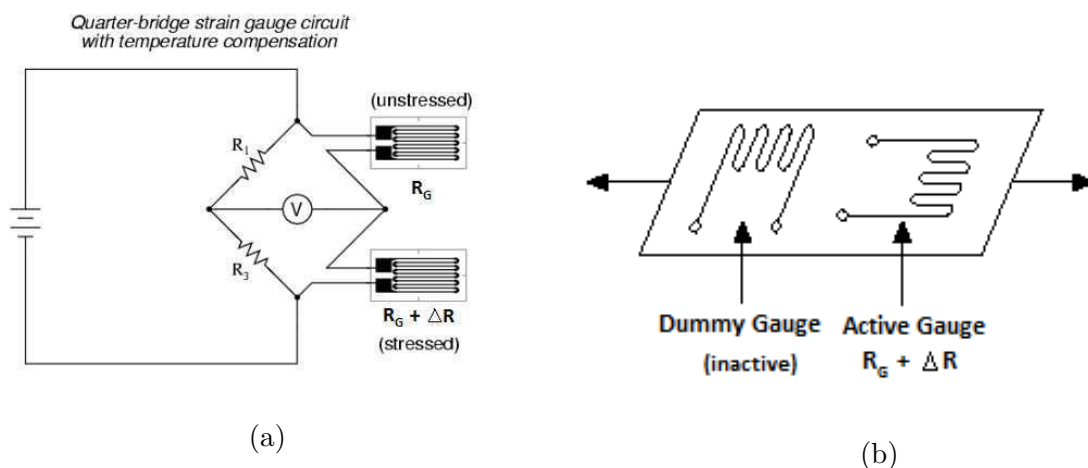


Figure 2.2: a.Wheatstone bridge circuit; b.Dummy gauge

The strain has little effect on the second gauge, called the dummy gauge. However, any changes in temperature will affect both gauges in the same way. Because the temperature changes are identical in the two gauges, the ratio of their resistance does not change,

the output voltage  $V_o$  does not change, and the effects of the temperature change are minimized.

As for the sensitivity, another design is used to double it by making both gauges active in a half-bridge configuration. For example, the gauge mounted on the upper side is in tension ( $R_G + \Delta R$ ) and the other underneath the beam is in compression ( $R_G - \Delta R$ ) Figure 2.3.

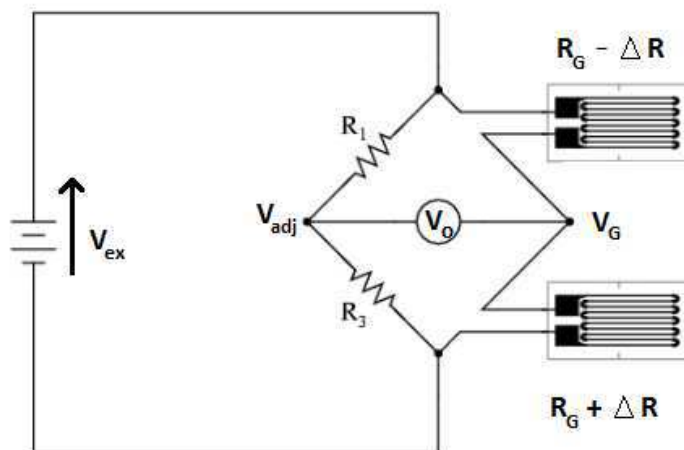


Figure 2.3: PushPull configuration

In this case the half-bridge configuration yields an output voltage that is linear and approximately doubles the output of the quarter-bridge circuit.

$$\begin{aligned}
 V_G &= \frac{R + \Delta R}{(R + \Delta R) + (R - \Delta R)} \\
 &= \frac{R + \Delta R}{2R} V_{ref} \\
 &= \frac{V_{ref}}{2} + \frac{\Delta R \cdot V_{ref}}{2R}
 \end{aligned} \tag{2.2}$$

Where  $V_G$  is at the voltage divider composed of the strain gauges while  $V_{adj}$  is at the other end of  $V_o$ . To balance the Wheatstone Bridge, the two other resistor  $R_1$  and  $R_2$  are adjusted to force the output voltage  $V_o$  to zero when there is no applied force ( $\Delta R = 0$ ). For that  $V_{adj}$  must be equal two  $V_{adj} = \frac{V_{ref}}{2}$ . the output voltage  $V_o$  is given by:

$$\begin{aligned}
 V_o &= V_G - V_{ADJ} = \left( \frac{V_{ref}}{2} + \frac{\Delta R \cdot V_{ref}}{2R} \right) - \frac{V_{ref}}{2} \\
 &= \frac{\Delta R \cdot V_{ref}}{2R}
 \end{aligned} \tag{2.3}$$

Table 2.1 summarizes some characteristics of the different types of Wheatstone bridge configurations.



Characteristics	Quarter bridge	Half bridge	full bridge
$V_o = 0$ when no load is applied	+	+	+
Limitation of the effect of wires resistances	+ (for the three wire configuration only)	+	+
Limitation of the temperature effect	none	+	++
Sensitivity	+	++	++++
Cost	+	++	++++

Table 2.1: Comparison of different strain gauge Wheatstone bridge configuration

### 2.1.1.2 Force sensing resistors-FSRs

Force Sensing Resistors (FSRs) are resistive elements whose resistance is a function of the force applied to a nearby/surrounding area. As force on the sensor is increased, resistance is decreased. Some FSR technologies use semiconductive elements [25] while others use carbon inked polymers.

FSR construction can generally be categorized into one of two types: ShuntMode and ThruMode which are illustrated in Figure 2.4. These two types are interchangeable in terms of basic functionality. However, these two types exhibit different Force vs. Resistance response curves, and are thereby preferable for different design applications. Shunt-mode is known to show a bit more dynamicity.

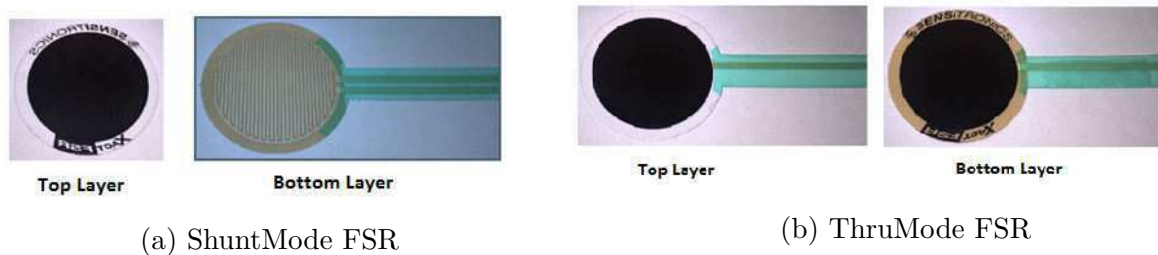


Figure 2.4: ShuntMode and ThruMode sensors

**ShuntMode** which is the most common construction mode. As shown in Figure 2.5, it includes mainly two layers in addition to spacer layers.

- The top layer of the FSR consists of a solid area of a semi conductive FSR element deposited on a flexible substrate, or of a polymer surface printed with carbon-based ink.
- The bottom layer consists of conductive traces(ex: silver or any other conductor),on a flexible substrate arranged into two sets of interdigitating fingers.

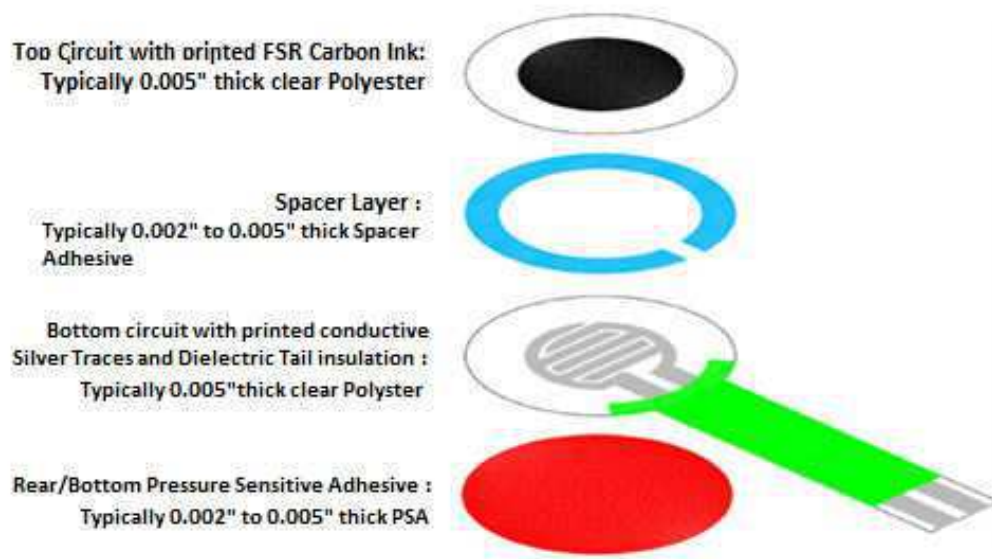


Figure 2.5: FSR layers in ShuntMode

When the two layers are pressed together, the semi conductive FSR element on the top layer shunts the traces on the bottom layer (hence the name ShuntMode). The resistance seen across the output terminals which will be connected directly to the bottom layer depends on the pressure applied to the sensor. The resistance seen across the output terminals which will be connected directly to the bottom layer depends on the pressure applied to the sensor.

**ThruMode** construction, illustrated in Figure 2.6 is based on one layer (or eventually two layers) of semi-conductive FSR sandwiched between two conductive layers. The solid conductor on each layer runs to a single output terminal, and any excitation current passes through one layer to the other, hence the name ThruMode.

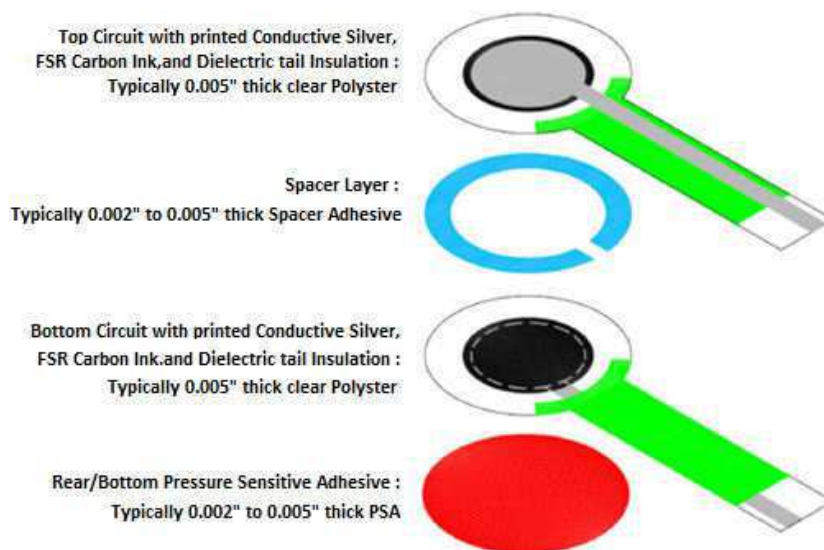


Figure 2.6: FSR layers in ThruMode

In case we use two layers the piezoresistive material is deposited on top of a solid conductive area (rather than interdigitating fingers), completely covering the conductor. This is done identically on both the top and bottom layers, which are then affixed facing one another.

In a ThruMode construction we either use :

- An intermediate of a solid semi-conductive *FSR* element as in FSRs provided by Sensitronics. They use this technology in both single *ThruMode FSR* elements and sensor matrices and arrays. This method is adopted by Interlink in their FSRs.
- Butler technologies ink use an intermediate polymer layer doped with carbon graphite particles. This layer is sandwiched between the two conductive layers. As force is exerted, the spatial configuration of carbon particles varies, the particles become closer to one another and the resistance decreases.

**Matrix arrays** Both *ShuntMode* and *ThruMode* technologies can be used to make multiple sensing elements arranged into one single matrix or array (For example, the matrix arrays provided by Butler technologies ink). See Figures 2.7 and 2.8 This technique is both exploitable and reliable when it comes to handmade FSRs. All that is needed is an elastic flexible material printed with conductive particles (carbon) and a couple of conductive sheets. Furthermore it's financially quite convenient.

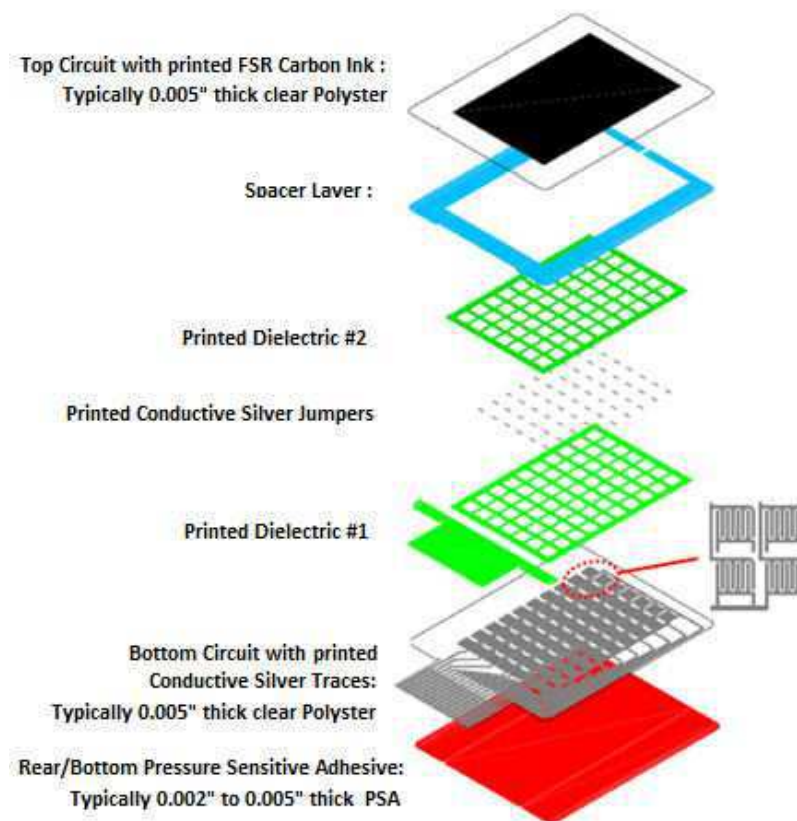


Figure 2.7: ShuntMode Matrix layers

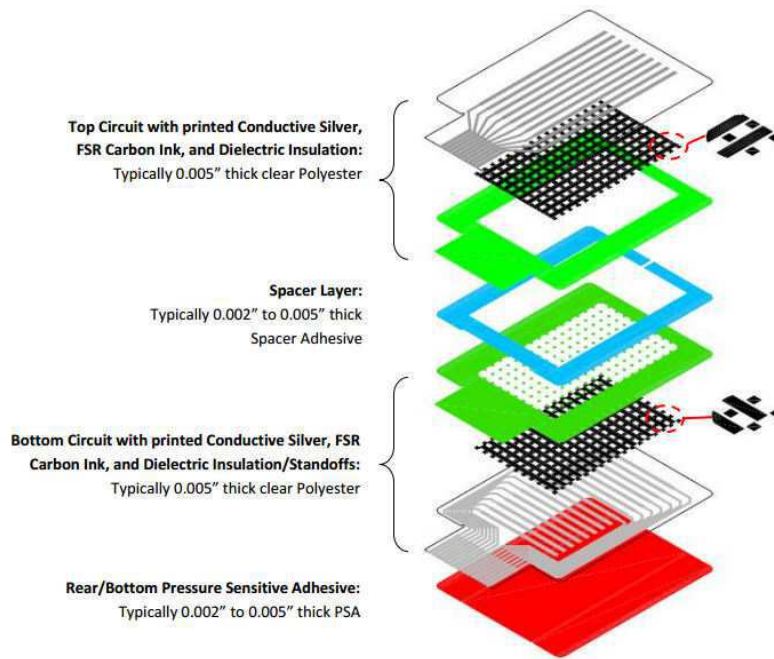


Figure 2.8: ThruMode Matrix layers

**Force and Pressure Vs Resistance** The diagram in Figure 2.9 illustrates how carbon-based FSR ink particles become compressed under increasing loads, resulting in the conductive particles being closer in proximity to one another allowing for a shorter conductive path leading to a lower overall resistance.

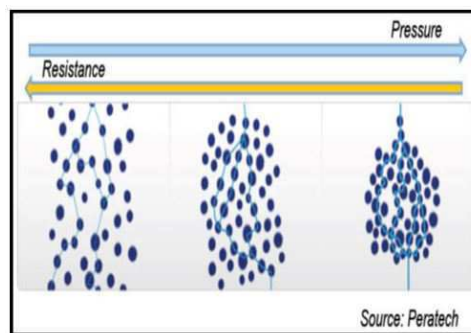


Figure 2.9: FSR ink particles when compressed

The variance of the resistance for all FSRs follows the same guise and differs from one FSR to another on the pace at which it varies as well as the range of loads it can operate for without breaking.

**Physical properties of an FSR** The mechanical properties of an FSR depend on the mechanical properties of the base material used for both conductive and piezoresistive layers. Generally different types of polymers are used. One common choice is polyethylene. A more solid version of it is the UHMWPE ( Ultra High Molecular Weight Polyethylene).

**Polyethylene** is an elastomer, a polymer with high Young's modulus and high failure strain compared with other materials. When it comes to application such as making a

force sensing tool it is important for our sheet to be elastic within the load range, durable and dynamic. Such characteristics are directly related to its young modulus, failure strain strength, etc (See Appendix B) All of This makes polymers like polyethylene both dynamicity and range wise qualified for our application. These information are prominent when choosing material to build an FSR system. The base-material must be chosen according to the systems requirements and usage circumstances such as maximum load and waterproofness.

### 2.1.2 Piezoelectric sensors

A piezoelectric sensor is a device that uses piezoelectric effect to measure the changes in pressure, strain, temperature or forces by converting them to electric charges. Piezoelectric effect can be used for various applications such as biomedical engineering, damage detection, automotive engines and electronics.[26] Piezo transducers are used as a sensors if they generate electrical polarization of material in a response to a mechanical action (Direct effect).However they act as actuators by displaying the mechanical deformation upon an application of electrical charge or signal (converse effect). There exist two types of this transducer according to the crystal used:

- Ceramic
- Polymeric piezoelectric materials

The piezoelectric ceramics such as PZT can be considered as a mass of minute crystallites, If the unit cell of the crystal lattice is such that the center of gravity of its positive charges does not coincide with that of the negative charges, it creates a permanent dipole. Polarization is observed if the dipole are aligned throughout the crystal.

As shown in Figure 2.10. In the direct effect, applying external mechanical stress will strain the dipoles, which alerts the polarization so the electric charges appear on the surface of the crystal. In the converse effect applying an external electric field will deform the natural dipoles inducing strain that change the dimension of the crystal [26]. The transducer made of ceramic have high modulus of elasticity therefore it can give a high frequency response. it has good linearity (less than 2%), low hysteresis (>1%) and it can be used to make a high special resolution array. [27]

The most suitable polymer material for clinically oriented body pressure measurement is polyvinylidene fluoride (PVDF) because it is flexible, thin and deformable [28], it has piezoelectric effect when polarized in an electric field, it overcome the relative fragility, poor fatigue resistance and cumbersome construction that were the major disadvantages of ceramic sensors. The charge developed on the surface of the piezoelectric material diminishes with time (leakage). Because of that leakage the transducer is best suitable for dynamic rather than static measurement.

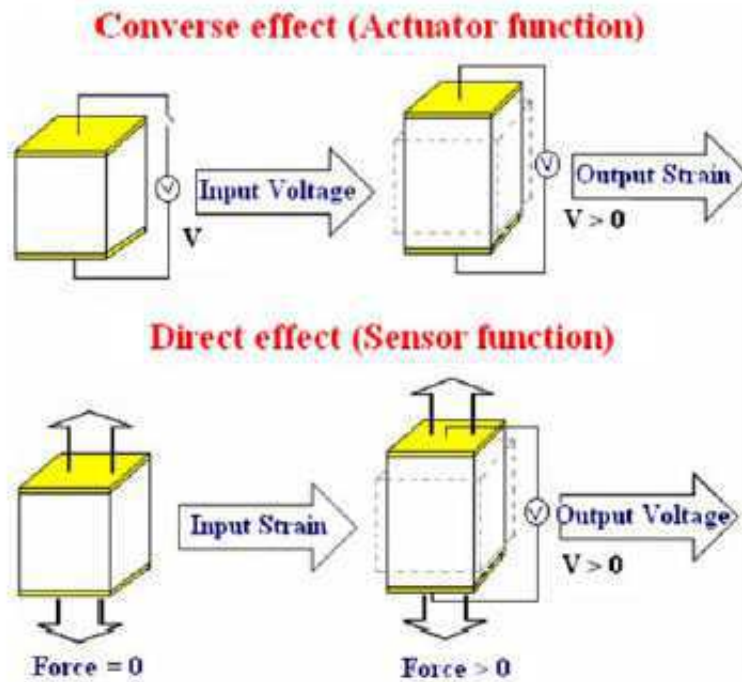


Figure 2.10: converse and direct effect

### 2.1.3 Capacitive sensors

Capacitive sensors are based on two conductive plates separated by a dielectric elastic layer. When there is pressure the dielectric is pressed or bent and the two electrodes approach each other. Capacitance changes since it is determined by the surface area and proximity of the conductive electrodes. This provokes a charge movement which creates an amount of electric current that is determined by the capacitance.

$$C = \frac{A * \epsilon}{d} \quad (2.4)$$

Where A is the area of each electrode,  $\epsilon$  is the permittivity of the dielectric and d is the distance between the two plates. Capacitive sensors can be fabricated in large arrays almost as easily as can a single sensor. Such an array was made from a rubber mat or an elastomeric dielectric DE, each side of which was covered by conducting strips, the strips on one side being placed orthogonally to the strips on the other side. The arrangement of strips in rows and columns allowed any point on the array to be sampled by selecting one appropriate strip on each surface. One arising problem is that a DE film exhibits large increase of capacitance when stretched but no significant enhancement with vertical compression. Böse, Fub, and Lux studied another design to enhance the sensitivity of the sensor in which they embedded the DE between two profiled surfaces (wave or knot profile). Figure 2.11 when the sensor mat is compressed the profiles penetrate into each other, stretching the DE film, thus the film thickness decrease and the electrical capacitance change. [29][30]

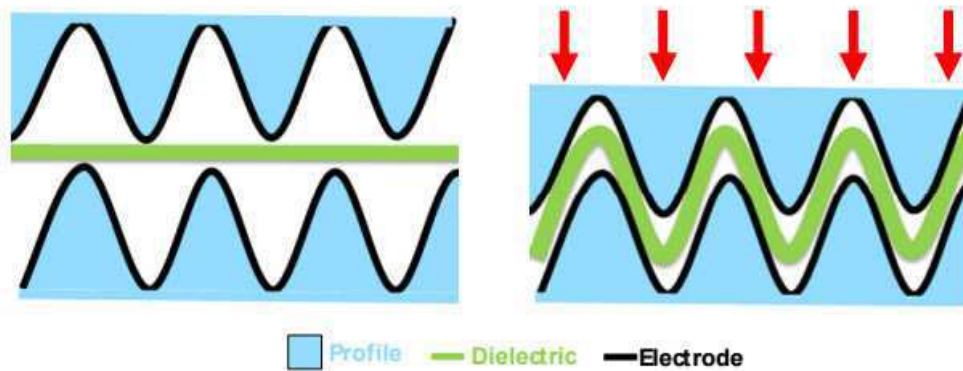


Figure 2.11: capacitive sensor with waveform profile

Capacitive sensing array can be used to make floor sensing systems. However, capacitive floor sensors present various disadvantages [27]:

- cross talk
- restricted frequency
- non-linear stress-strain
- mechanical hysteresis

## 2.1.4 Optical technologies

Numerous optical technologies can be used including pedobarographs and Bragg Fiber Optical sensors.

### 2.1.4.1 Bragg Fiber Optical sensors FBG

Another means of transducing force is the use of optical fibers. The most common sensing element for fiber-optic sensors is based on fiber Bragg gratings (FBGs), a technology originally developed to multiplex signals in optical networks.

Fiber Bragg grating is optical fibers that act like an inline optical filter against certain wavelengths. Manufacture of grating is created by exposing the fiber core (germanium-doped silica fiber) to a periodic pattern of intense ultraviolet light. The exposure produces a permanent increase in the refractive index of the fiber's core, creating a fixed index modulation according to the exposure pattern. This fixed index modulation is called a grating. When a light beam is sent to the FBG sensor, reflection from each segment of alternating refractive index interfere constructively only for a specific wavelength of light, called the Bragg wavelength given by Bragg condition described in equation

$$\lambda_b = 2n_e \Lambda \quad (2.5)$$

where  $n_e$  is the effective index,  $\Lambda$  is the spacing between the gratings, known as the grating period (see Figure 2.12)

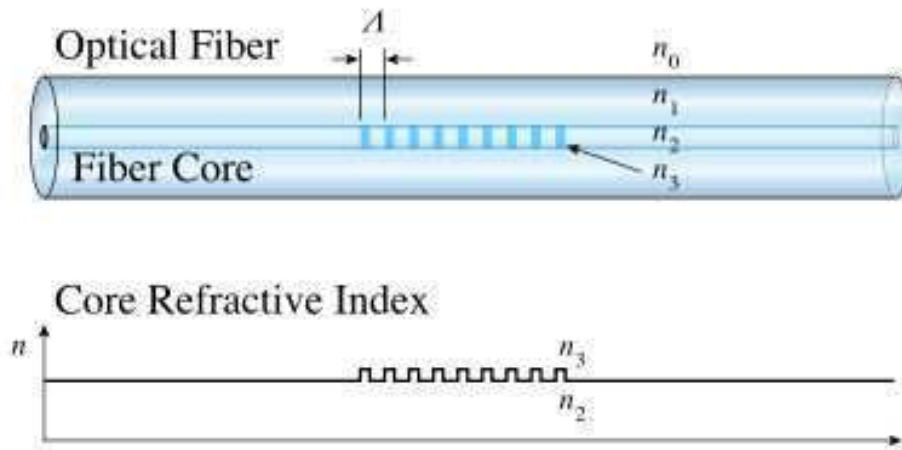


Figure 2.12: A Fiber Bragg Grating structure, with refractive index profile

When the FBG sensor is subjected to external mechanical perturbation (strain or pressure) the back-reflected peak wavelength will be shifted as illustrated in Figure 2.13 and that is according to the range to which the external perturbation influence the FBG.

A mechanical perturbation produces an axial strain. As a consequence, the spacing of the periodic variation  $\Lambda$  and the effective index  $n_{eff}$  changes, thus the Bragg wavelength change too.[31] ,[32] ,[33],[34],[35].

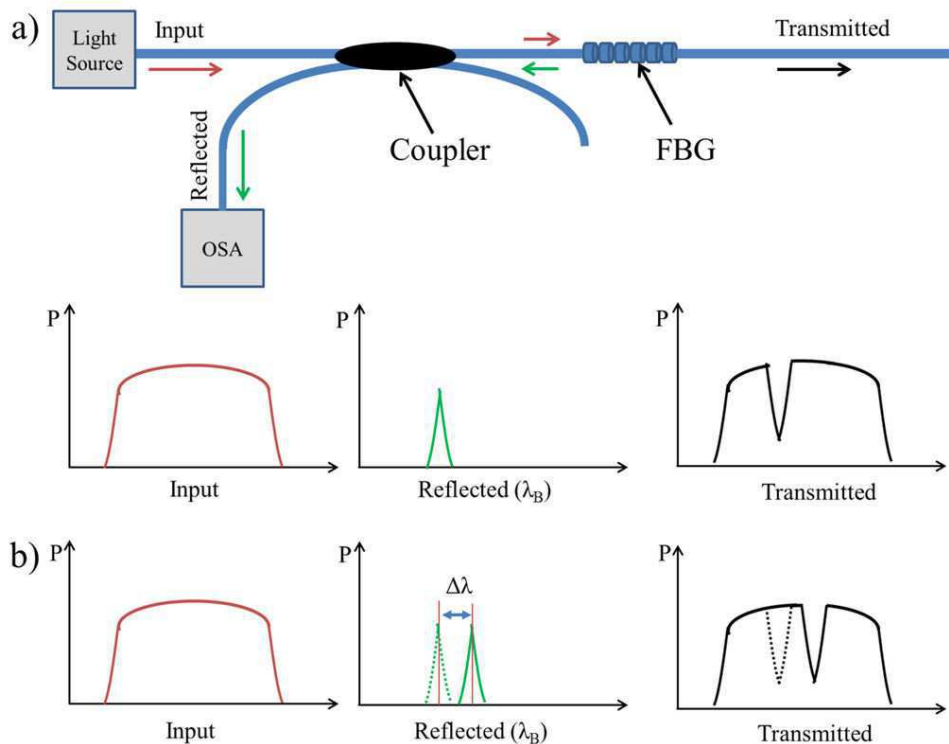


Figure 2.13: spectrum response of FBG

## 2.2 Comparison and technology selection

Selection is based on a set of desirable metrological characteristics which include:



- good spatial resolution (<1.5cmx1.5cm)
- Adequate Load range;
- good sensitivity ;
- High dynamic range.
- low hysteresis;
- low cost.
- Accessible fabrication procedures

First, optical fibers are excluded for accessibility reasons. Piezoresistive sensors present a broad bandwidth, can be cut in different shapes but cannot measure static forces. They are also the most expensive to manufacture (they must use charge amplifiers which can be costly to implement )

Capacitive sensors, despite being small and inexpensive, have various disadvantages including cross talk between adjacent capacitors, non linearity, limited by the thickness of the capacitive material and restricted frequency response.[27] Note that this is not a state-of-the-art case. Capacitive sensors, along with FSRs, are nowadays the most used pressure sensors for different application including plantar systems.

Another approach is to use strains gauges to build a multi-tiles platform designed to be as much of a high resolution as possible to fit into a pressure measurement platform instead of one rigid forceplate. That is the reason the number of load cells was brought down to one per 4-tile-intersection. However, Adopting this technology was unfortunately not possible and that is due to the fact that

1. The smallest available load cells that can meet the load range requirements are too big to fit into a high resolution system. Systems based on strain gauges are generally designed to analyze a jumping cycle (velocity, height ,etc).
2. Small load cells have small ranges (maximum of 10 kg) which makes them inadequate for this application.

Consequently, a second option which was to use FSRs was adopted. FSRs can be used in a configuration similar to those using load cells:4 FSRs for each tile. [36]

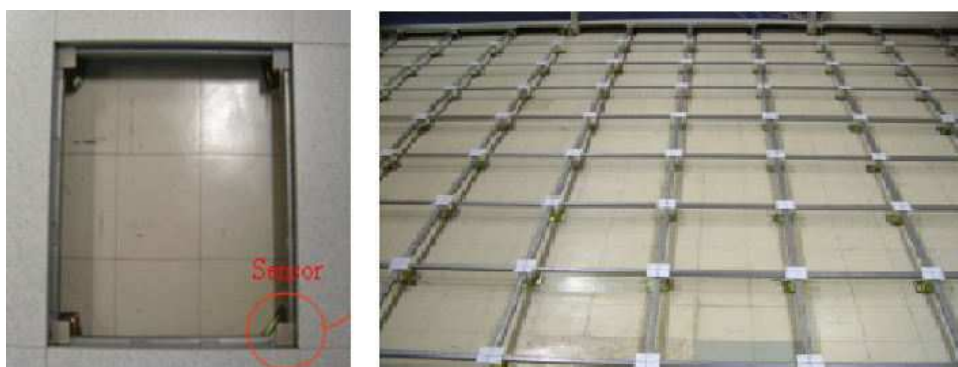


Figure 2.14: structure of a floor using FSR [36]

Other configurations can be applied such as in the pressure mat offered by brands such as Tekscan Technologies which is similar to that of the ThruMode matrix array provided by Sensitronics.

Comparing the different configurations relies on taking into account the following criteria:

1. load range in reference with the size;
2. algorithmic complexity Vs real time data visualization;

For instance, it can be seen that the first configuration is economic but requires heavy algorithms that are prone to weigh down the system when it comes to real-time analysis. The second approach seems practical so far but the load range is still to be discussed. In the last case we're no longer talking about a rigid force platform but a flexible mat which is much more practical in terms of unobtrusiveness and transportability

As for the sensing elements, different electric hardware providers offer a collection of pressure measuring resistive tools which come in several shapes: Interlink offers a set of singular FSR elements that are accurate to some extent ( $\pm 10\%$ ) but the FSRs both come in size too big to fit into a matrix array and have a small load range. See section 2.1.1.2

presents a major financial inconvenience which resulted in the adoption of a final solution that was to build the sensor array from the scratch, taking into account the specifications mentioned above.

## 2.3 Calibration

The overall performance of a sensor is based on its static and dynamic characteristics. Static calibration is performed at a certain input frequency (it can be null) as to get an input to output, while dynamic calibration describes the sensor's frequency response i.e. If the sensor is made to measure constant or slowly varying quantities, its performance can be evaluated with only the static characteristics. The dynamic description is necessary if we need to measure rapidly varying quantities. In such type of calibration, it must be taken into account that not only the sensors but also all the measurement system present a dynamic behavior. Consequently, dynamic characteristics of the measurement system must be known. It is recommended to make sure that the operating frequency range is within the bandwidth of each of its components. Most cases sensors are calibrated in both dynamically and statically methods for comparative study to satisfy the identity between the static and dynamic sensitivity of the sensor. An example can be seen at [37]

A pressure sensor can be calibrated statically by using a known weight under a static conditions and thus the exerted force is calculated using the ground reaction force  $F = M.g$  that is eventually divided by the surface of the sensing area. Note that it is important to distribute load equally over the surface as to get homogeneous pressure.

However, looking at the frequency and velocity of walking it is easily noticeable that fast variation of the detected pressure at each of the sensing elements of the mat ,regardless of their type, is frequent. Therefore, the dynamic behavior of these sensing elements is of great importance. Dynamic calibration is done using a periodic or an aperiodic excitation.

### 2.3.1 Dynamic calibration methods

**Periodic calibration** [flexiforce] performed a dynamic calibration in a study of their flexiforce sensor using periodic generator. Their equipment consisted of an oscillating mass with an accelerometer board mounted on it, a plastic frame fixed at a head of a shaker which is excited by a function generator and power amplifier units to generate an excitation with various frequencies, amplitudes and function shapes. See Figure 2.15.

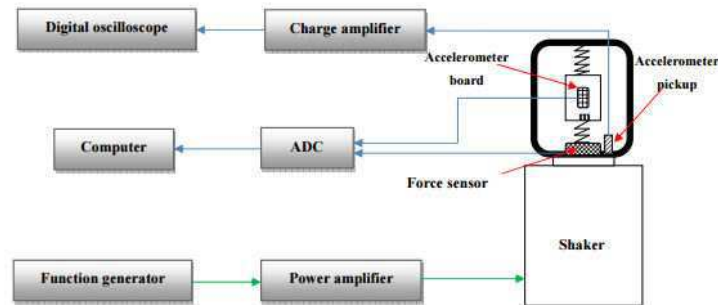


Figure 4. Calibration instruments connection scheme

Figure 2.15: Dynamic calibration with periodic shaker

**Aperiodic calibration** The Figures 2.16 above illustrate the calibration methods that use a step function

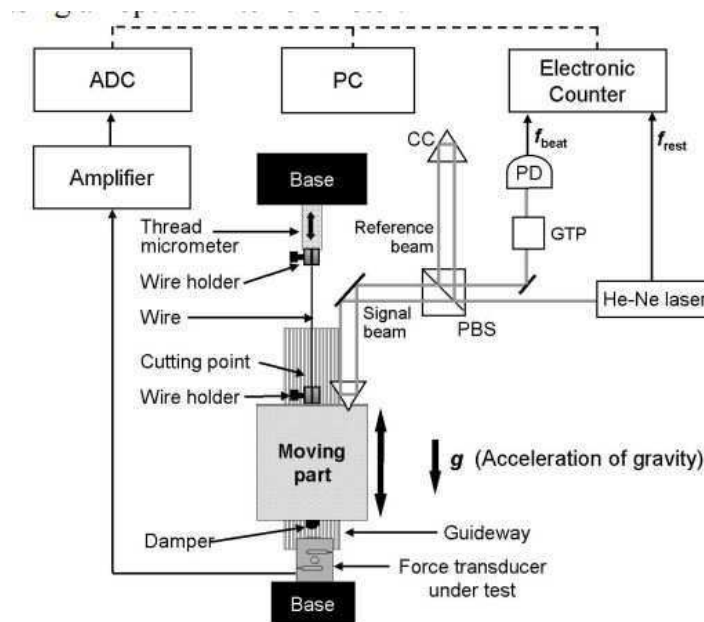


Figure 2.16: Step Force Calibration

A mass  $M$  is suspended using a stainless steel wire, just above a force transducer under test. The initial distance between the object and the force transducer is adjusted using a thread micrometer attached to the upper base. A perpendicular motion with small friction is released by using pneumatic linear bearing. The data is measured from the transducer after dropping the mass by cutting the wire and the inertial force acting on the object is

measured with high accuracy and that is by measuring the velocity of the mass using an optical interferometer.

### **Conclusion**

This chapter discusses different state-of-the art pressure measurement technologies. These technologies are then compared in terms of accuracy, size, simplicity and cost. Consequently, force sensing resistors are chosen for the project. Next was the study of the basic structure of an fsr from which was derived the basic model for our pressure platform which will be basically a Thru mode FSR matrix. This structure is the same used by Tekscan Technologies, Black butler and Sensitronics.

## CHAPTER 3

# Chapter 3

## Conception and Engineering

This chapter gives a detailed description of the project. The conception process relies on a top down method. That is starting from an idea, then using the accessible tools to build what we call a proof of concept i.e. a prototype built to test a concept or process or to act as a thing to be replicated or learned from.

### 3.1 Basic structure

Our system mainly comprises:

1. A floor sensing equipment: designed based on a FSR matrix array technology. The design was inspired by the study of different FSR sensing systems.
2. A data acquisition system: That includes all the electronics necessary for conditioning, treatment and processing of the collected electrical output of the sensing elements.
3. A user-friendly interface that allows to visualize collected information and display them in the simplest and most comprehensible way possible.

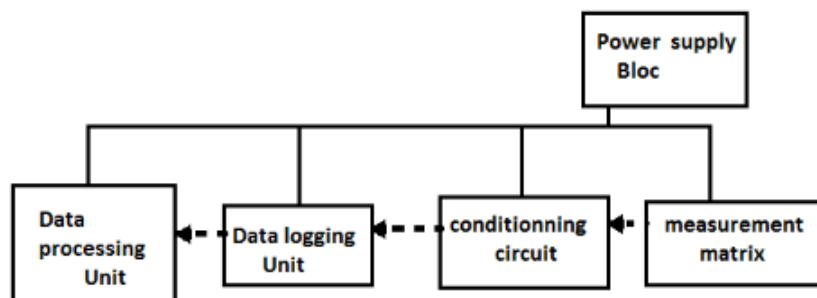


Figure 3.1: Block diagram

### 3.2 General description of the mat

The basic structure of the sensitive layer of the mat was drawn from studying the general structure of several FSRs and sensor matrices. It is to some big extent similar to the basic structure of the sensor matrix produced by Sensitronics and also similar to the pressure

mats produced by Tekscan .

The pressure mat consists of a total of 5 layers that serve different purposes. The arrangement of these layer is shown in Figure 3.2;

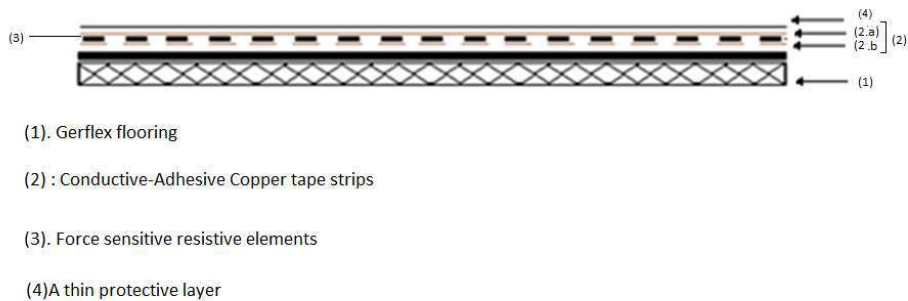


Figure 3.2: Side view of the pressure mat

1. **Base layer:** constitutes the majority of the mat. It should be neither rigid nor elastic. Otherwise it would alter the measurements.
2. **Conductive adhesive copper stripe:**It is important for these strips to be backed by a conductive adhesive which provides electrical connection between its two sides. The strips on one layer run orthogonally to the strips on the opposite layer.
3. **Protective layer :**it must be flexible in order not to get cross-talk effects
4. **Piezoresistive material-*Sensing Resistive Layer (LSR)*** The mat comprises a 0.4mm layer of Polymer Carbon mixture developed by Andrew Clark [38]. A polymer film UHMWPE (ultra-high molecular weight polyethylene) injected with a certain concentration of carbon graphite particles to make it conductive. This material from sensor film kit [39] comes in sheets of 4" x 6" Figure 3.3 that we cut into 0.7cmx0.7cm squares, each of which are sandwiched between the two stripes layer at each intersection. The sensing square elements are spaced by 0.7 cm horizontally wise and 1 cm vertically using a dielectric (air for instance). Each resistive rectangle defines a 1.7cmx1.4cm pressure cell (PC)



Figure 3.3: 4" x 6" Sensor Fil Kit

- *Electrical characteristics:* conductivity is defined by how spaced the graphite particles are. The bigger the applied pressure, the closer are the carbon particles and the more conductive the material becomes. (The lower the resistance).

- *Mechanical characteristics:* Even though this material presents a high young modulus which might results in a low sensitivity, some properties that makes it best suitable for our applications. These properties include :

- Excellent abrasion resistance
- A high tensile strength at yield(among the highest of plastics) [40] No failure risks within our pressure range 0-1.6 Bar (see section1.1).This sheet of film is used by Andrew clark to make a smart mat that goes under door mats and detects the weight of people or pets and triggers actions [41] .

There exists another type of conductive polymers (also injected with carbon particles), called Velostat but it presents a much lower yield limit.

- Superior chemical resistance even to the most aggressive chemicals. Greater chemical resistance than steel and nylon.
- Water repellent highly resistance to hydrolysis
- Stress crack resistant

- *Dimensions:* The floor mat's sensitive area (indicated on the surface) is 178.5cm long (105x1.7) and 39.2 (28x1.4) wide. A single sensing cell is 1.7cm long and 1.4 cm wide. Note: The limitation in the number of the pressure cells is due to a shortage in the piezoresistive material.

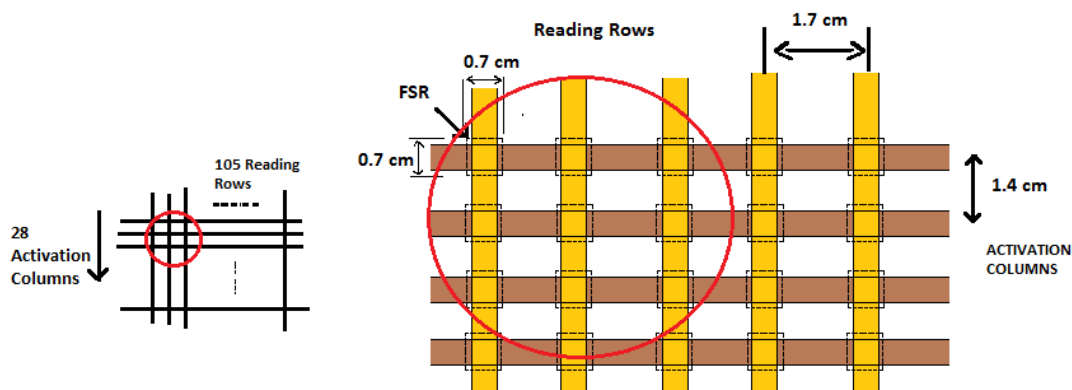


Figure 3.4: top view

### 3.3 How does it all work?

#### 3.3.1 General Mechanism

The primal sensing element is the middle layer. Its conductivity depends on how spaced are the graphite particles. The bigger the applied pressure, the closer are the carbon



particles and the more conductive the material becomes. The top conductive layer (2.a) in Figure 3.2 comprises a set of 105 copper strips spaced by 1.2cm. Let's name them "reading rows" while the bottom conductive layer (2.b) consists of 28 copper strips spaced by 0.9cm, let's name these "activation columns". The stripes on the top layer run orthogonally to the those of the bottom layer such that at each "remote" intersection of rows and columns, a resistive element from the middle layer is placed between the two conductors. One scan of the pressure mat is the measurement of all the FSRs. Row by row and columns by column.

For each FSR, the principle is simple: Resistance is determined through a voltage divider output collected from across a parallel resistor of  $R_p = 1M\Omega$  which is placed at the end of each reading row and at the entrance of the analog read pin of our measurement system. To measure resistance from row  $i$  and column  $j$ . row  $i$  is selected (voltage will be measure across resistance  $R_p(i)$ ) and column  $j$  is set to  $5V$  Figure 3.5. The collected voltage allows us to calculate the resistance value at the selected pressure cell. Then, we can determine pressure based on calibration of the sensing elements.

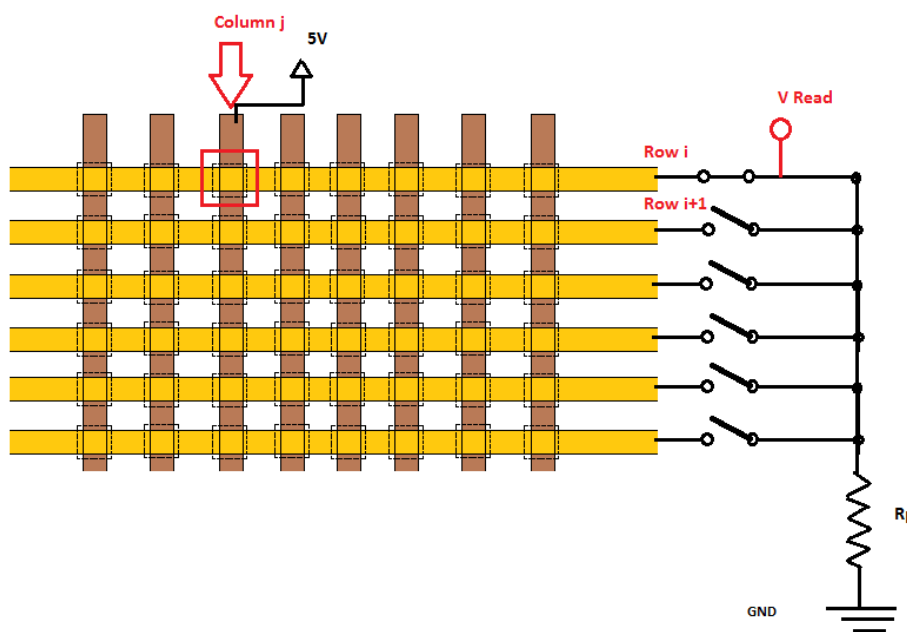


Figure 3.5: Functioning Principal

One scan is done by reading voltages from rows one by one such that each of voltages collected from one row corresponds to the activation of a given column that corresponds to one particular FSR element.

A collected voltage is transmitted to the data "acquisition" board which will determine the resistance (Hence the pressure) at a given PC (pressure cell).

### 3.3.2 Row Selection

Reading rows are multiplexed using seven 16 to 1 4076 CMOS based Multiplexer. all the output are connected to each other and one output of one multiplexer is selected at the

time.

The selection of a given multiplexer is done by activating it and deactivating the others. These multiplexers are activated by setting there Enable ( $\overline{EN}$ ) pin to "0" (GND). This is done connecting these pins to outputs of 1to8 channels 4051 module as a demultiplexer. Pull up resistors are connected to these outputs such that the input is connected to GND See Figure 3.6.

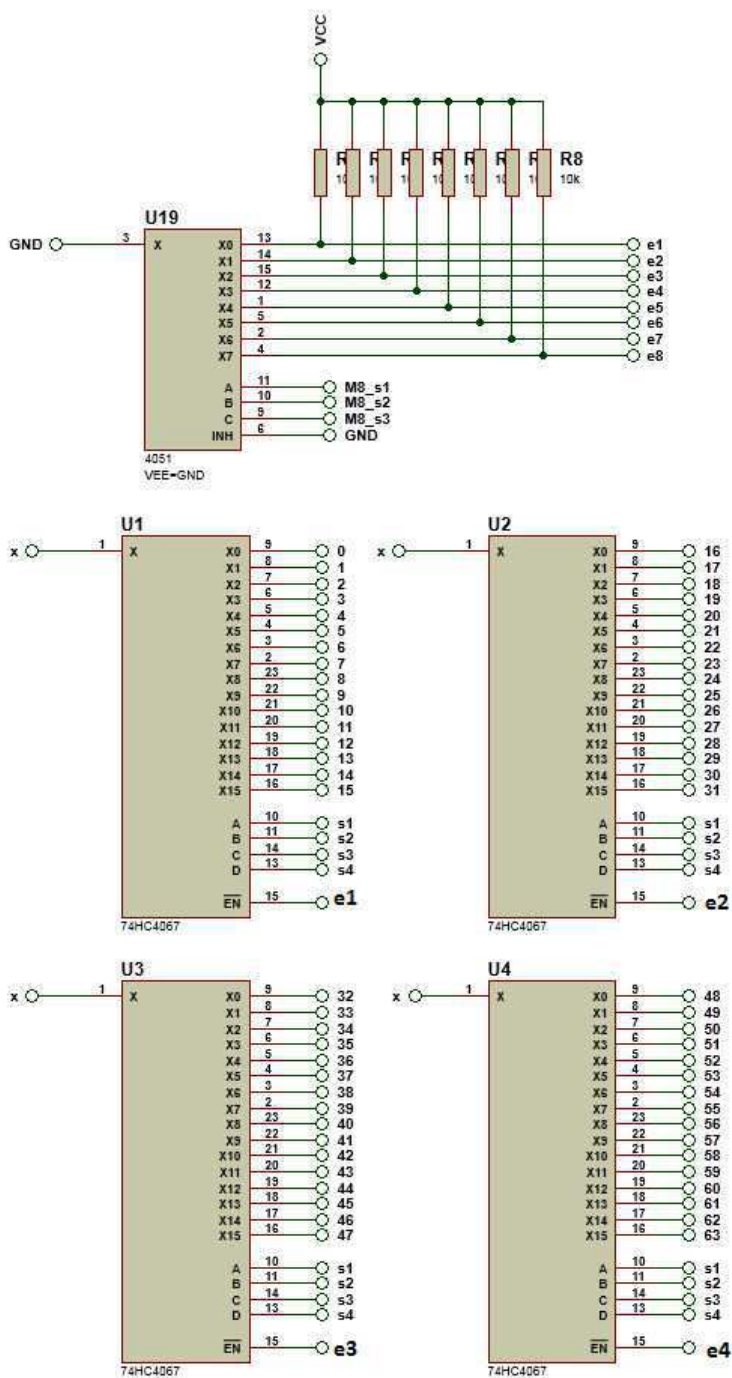


Figure 3.6: Row Read

### 3.3.3 Column selection

A first approach is to use 1-to-16 4067 modules as demultiplexer with their outputs connected to their respective columns Figure 3.7. A 4x4 matrix simulation is carried out using Proteus 8.4, which offers a large set of libraries including an Arduino library which allows us to simulate the system.

An Arduino UNO board is used as the processing unit

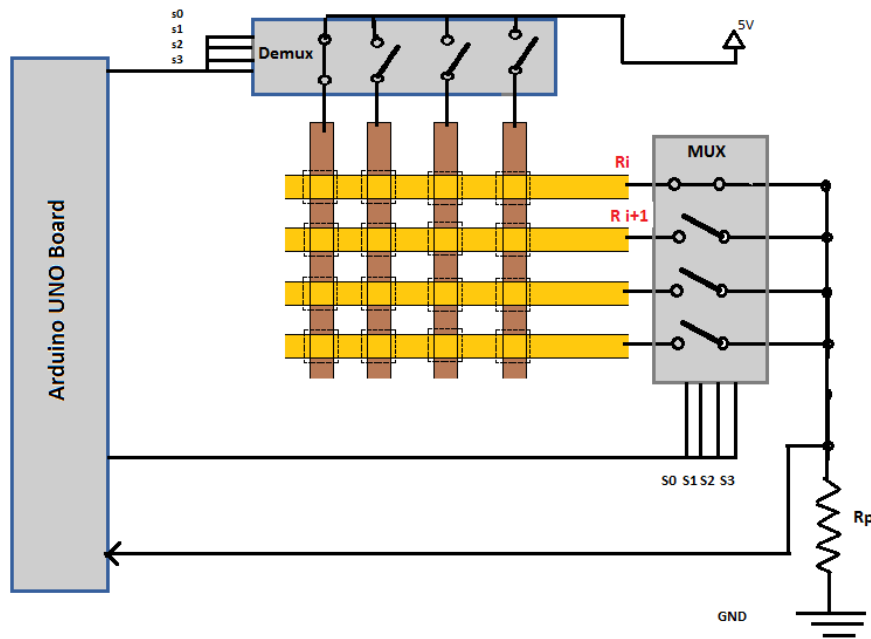


Figure 3.7: Column selection using 4067 Demultiplexer

Two major issues come into sight: Ghosting and data interdependence.

**Ghosting:** "Ghosting" is a term that describes a common issue that arises in sensor or button matrices. Let's suppose that pressure is applied to the 3 pressure cells indicated by the 3 red circles. A non-pressed pressure cell is electrically similar to an open circuit.

The schema in Figure 3.8 demonstrates a typical ghosting situation: Column 1 activated. While column 2 is disconnected. (in a way set on high impedance).

The Microcontroller starts scanning the rows one by one. Note that current will flow as indicated from one point to another and that is only because *the voltage is decreasing from one point to another in a closed circuit*. The system will indicate that the non-pressed cell is pressed (as we're activating column 1 and reading row 2) which is a ghost information (it doesn't exist but it appears in the results)

In short, the issue is that when multiple cells are pressed, unintended paths between rows and columns can be created, resulting in false readings on a non-pressed cell.

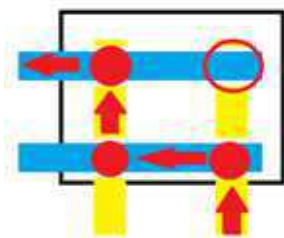


Figure 3.8: Ghosting

**Data interdependence:** Voltage measured for a certain FSR changes if we vary any other FSR from the matrix Figure 3.9. (A simple Thevenin representation of the impedance across the terminals of the selected FSR can confirm it ).This will result in either a set of 2940 variables equations to solve in a very short amount of time. Or, A reading error that might reach up to 90% (for 2 x 2 grid).

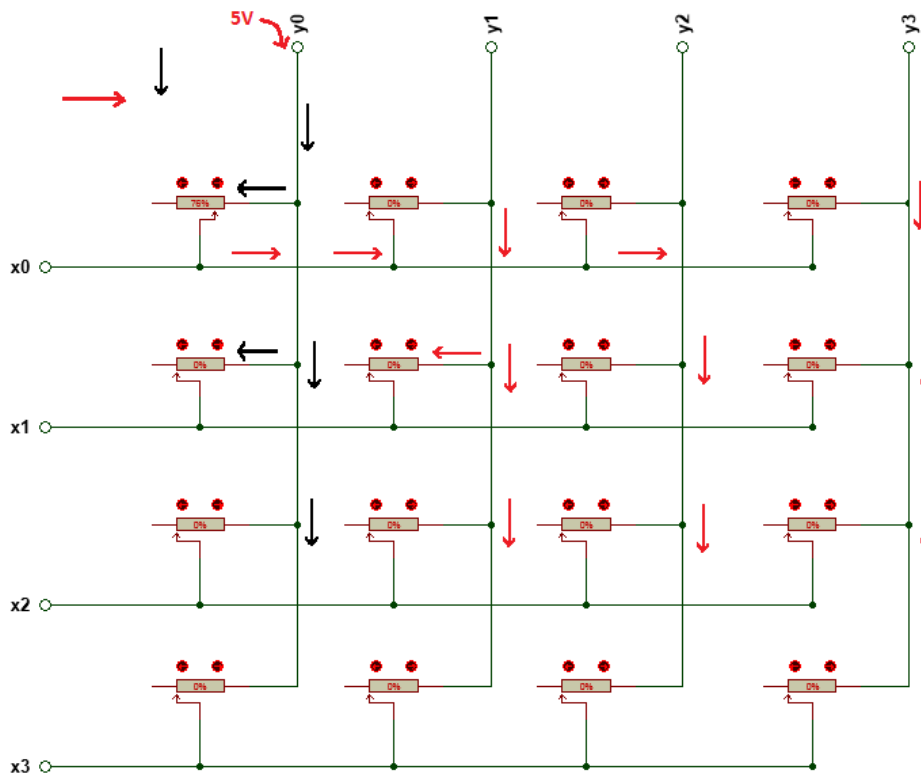


Figure 3.9: Illustration of the data interdependence in a mux-based activation case

The following illustrations Figure 3.9 demonstrate a case of a 4x4 equivalent circuit of a 4x4 FSR matrix (Y0, y1 , y2 , y3 represent the activation columns. Red arrows indicate the undesirable current flow)

**Solution :**

**Theory:** Looking closely at the circuit, it can be seen that setting the inactivated columns to a voltage lower than the activation voltage value eliminates the effect of Fsr on the rows that are not selected.see Figure 3.10.

Current cannot flow from the selected row to the other rows and vice versa. Therefore, A shift register is used and that is to ground the columns that are not activated and set only the activated column to HIGH VALUE (which in this case is 5v).

It is clear that voltage recorded for a particular PC on a particular row depends only on the FSRs from the same Row.This results in a significant decrease of the number of variables being part of the processing of one single FSR to a maximum of 28 variables.This technique also allows to eliminated ghosting. Current flows naturally from a higher voltage to a lower voltage. This how ghosting is eliminated. see Figure (3.11)

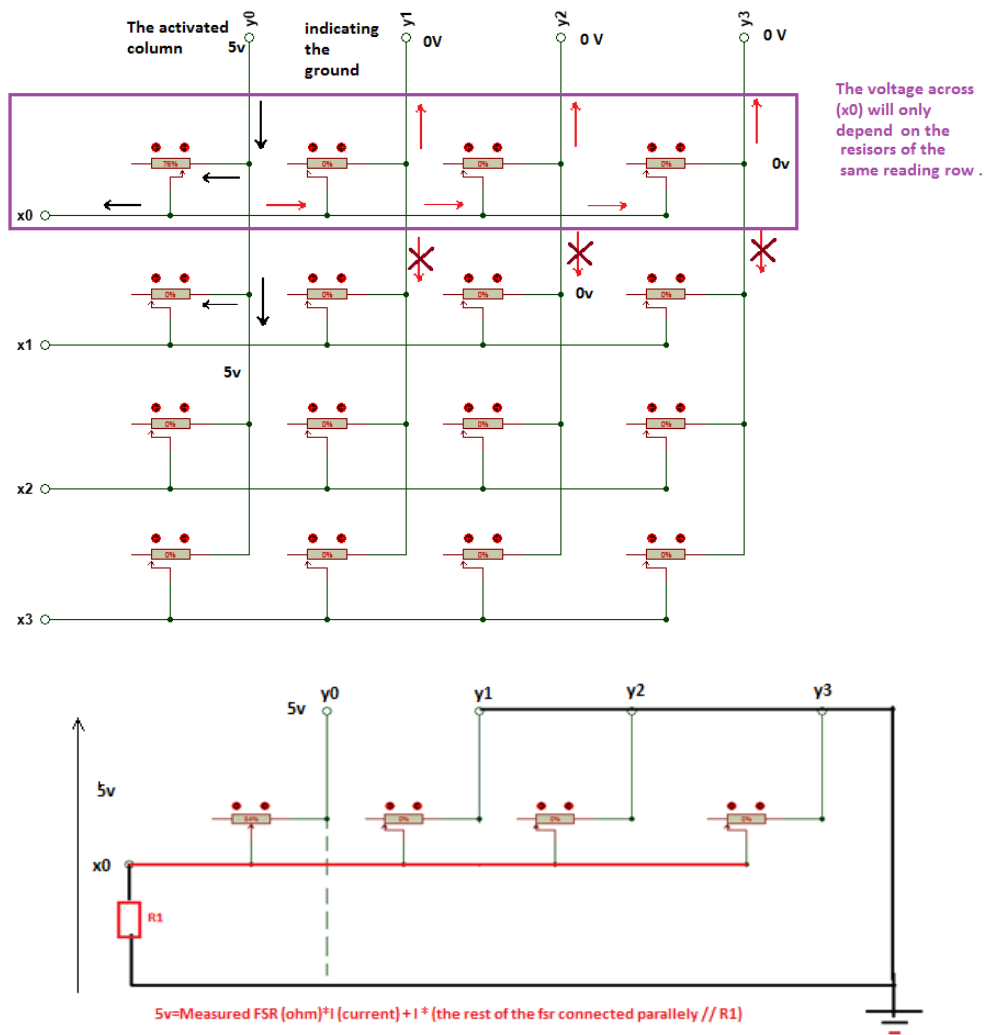


Figure 3.10: illustrated Solution for data inter-dependence

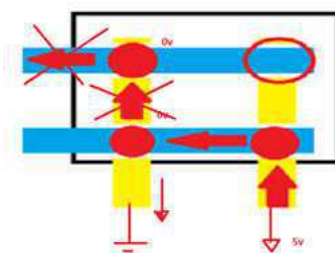


Figure 3.11: Ghosting elimination

Consequently, the drive columns are connected to 4 cascaded 74-HC595 shift registers through their parallel outputs. A single impulsion of 5V will be generated at the beginning of each row scan and then shifted to activate the columns one by one successively. For each row, the respective output voltages are collected and used to calculate the corresponding FSR values.

### 3.3.4 Buffers

At first, simulation of the system is done using Proteus 8.4 Professional a 3x3 matrix combine with two 74HC4067 Multiplexers and two 74HC595 shift registers. see Figure 3.12.

The Arduino code used in the simulation is taken from a tutorial by Sensitronics in which they test matrix arrays.

**Observation:** The shift registers outputs that the columns are activated one by one while the other columns terminals are set to 0V. Voltage collected for a given FSR measurement depends on only FSRs from the same row. However, it observed that shift registers delivered activation voltage depends on the FSRs of the selected row.

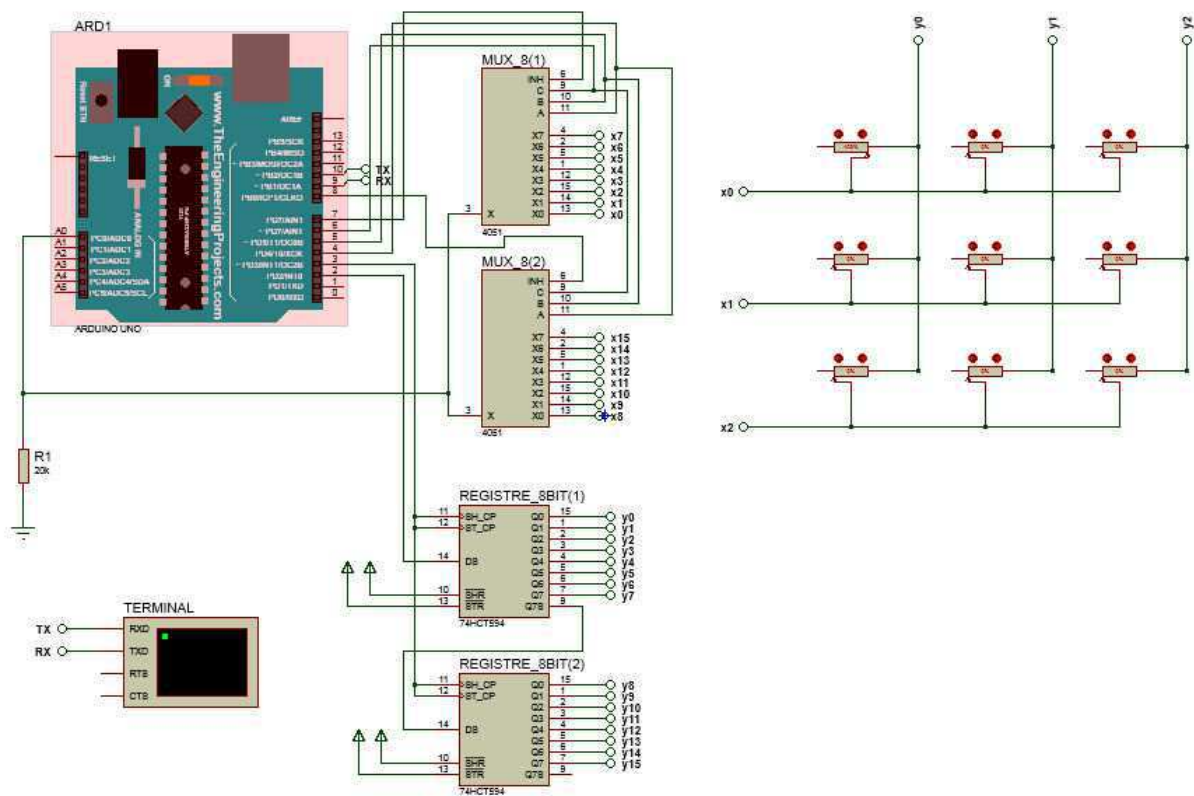


Figure 3.12: Simulation with no buffers

**Solution:** A solution is to use buffers. A buffer is any four-terminal characterized by an infinite input impedance, an output impedance no greater than a few tens of ohms and an Input voltage equal to output voltage regardless of the impedance on both ends of the two-terminals.

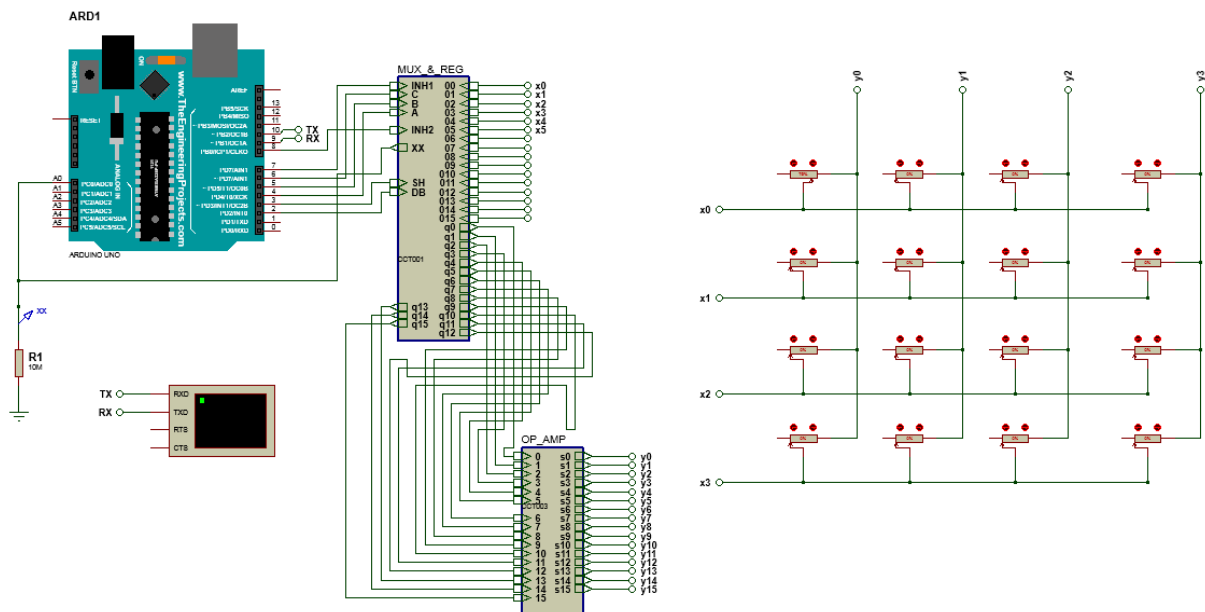


Figure 3.13: Simulation with buffers

An example of a buffer that is used in our system is voltage follower. An operational amplifier is placed in front of each activation columns such that the output is connected to both the inverting input and the corresponding activation column while the non-inverting input is connected to its respective register's output. This guarantees an activation voltage of 5V regardless of the values of the matrix FSRs. A 4x4 sensors system is simulated. Figure3.13

*Results:* the problem is solved and The current design of the conditioning circuit can be validated. Note that it is also possible to eventually add an amplifying stage as to amplify the collected voltage. However the resulting voltage has to be within the input range of the data acquisition unit.

### 3.3.5 Determining FSRs from the same Row

#### Reducing the number of variables

A small experiment have been done on 3 sensing  $0.7cm \times 0.7cm$  sensing elements where the following remarks have been drawn:

1. If a PC (pressure cell) is not pressed the sensitive elements proved to show resistance that can be assimilated to an open circuit ( over  $100 M\Omega$  ). In our system ,this results in a collected voltage that is negligible to that when the PC is pressed. (Current is practically equal to zero)
2. If a PC is pressed , Resistance drops significantly to a value of below 20 M. This corresponds to a jump in the collected voltage value. Therefore, it is possible to select the pressed cells by com paring the corresponding read voltage to a threshold value. Only these elemen ts have to be calculated. The rest of the pressure cell are supposed to own a value of over  $100M\Omega$ . Thereby, the number of variables is brought t down to the number of the pressed cells.

**Solving the Equation set** For each row, Collected voltage corresponding to a pressed pressure cells is stocked and used to calculate the value of their respective resistances and represent their corresponding pressure values . This results in an N-set of non linear equations with N variables to determine. The equation set is solved using Newton-Raphson iterative method. (see appendixA).

### 3.3.6 Data acquisition

- **How fast?:** Ideally the system is to be scanned at a frequency of 120 scans/sec [see section 1.3]. With a total number of 2940 sensors the system will have to collect voltages at 352,8 KHz. Thereby, An electronic board of a high acquisition rate must be used

The collected data is then processed by the microcontroller. Processing is either done in real time or divided such that collected data is logged to be processed but not entirely in real time. It all depends on the capacity of the microcontroller in terms of clock rate, Cache memory, RAM memory ,etc.

We can also use one board for data acquisition and connect it to a more powerful processing unit for heavier operations.

- **”Analog read” requirements:** For the data acquisition board, any board with input analog pins adequate for sensor readings would do. However there is a select number of characteristics that needs to be considered when choosing a board.
  1. Reading resolution which is due the size of the ADC converter output . The ADC is generally mounted into the pin’s circuitry.
  2. Input voltage range: defers from one board to another .
  3. The choice of the reference voltage which is the voltage that corresponds to the maximum binary generated by the ADC.
  4. The dynamicity of the ADC regarding the output impedance, the input circuitry generally comprises a sample and hold circuit whose charge time constant depends on the output impedance.
  5. Accuracy and repeatability which can also be altered due to misconnections across the circuit , ground loops noise ,etc. Inaccuracy tolerated in this case depends on the pressure scale resolution used for the foot print detailed display.

### 3.3.7 General structure

A board equipped with an input analog pin (in addition to at least 9 digital input output pins )is used to read the collected value and monitor multiplexer and registers to synchronize the scanning process as described in section (3.2.2). Two DAQ boards available at the department are : Arduino UNO or a NI USB-6002.

It receives commands through an appropriate software interface installed on computer which handles the data processing part.



### 3.3.8 Software Application

#### 3.3.8.1 Arduino interfaced with MATLAB GUI

MATLAB support package for Arduino makes it possible to write MATLAB programs that read and write data to the Arduino through a serial interface. Because MATLAB is a high level interpreted language, programming with it is easier than with C/C++ and other compiled languages, and one can see results from I/O instructions immediately –no compiling. MATLAB includes thousands of built-in math, engineering, and plotting

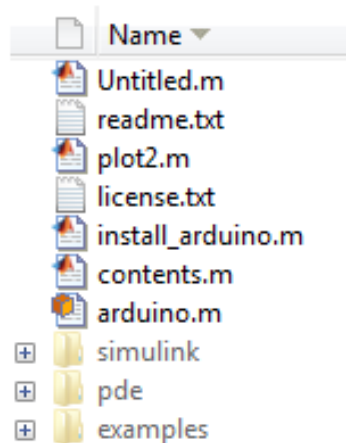


Figure 3.14: Matlab Packages for Arduino

functions that we can use to quickly analyze and visualize data collected from our Arduino. Furthermore MATLAB GUI allows to create an interface for the systems application.

#### 3.3.8.2 LabView

LabVIEW is a highly productive development environment for creating custom applications that interact with real-world data or signals. Programming is based on intuitive, flowchart-like graphical dataflow programming model known as "G programming" or "LabVIEW programming" in which nodes (operations or functions) operate on data as soon as it becomes available rather than the sequential line-by-line manner that most programming languages employ. It also includes:

- A DAQ module which serves as an interface between the NI USB- 6002 Board or any other board from NI. and our application's processing code .
- All kinds of tools for numeric statistical, logical operations for matrices of all dimensions and data types.

### 3.3.9 Arduino uno VS. NI USB-6002

Aspects that are mostly taken into consideration when comparing the two boards are accuracy and data acquisition rate.

#### 3.3.9.1 Technical specification

**Arduino Uno R3** : is a microcontroller board based on a removable, dual-inline-package (DIP) ATmega328 AVR microcontroller. It has 20 digital input/output pins (of

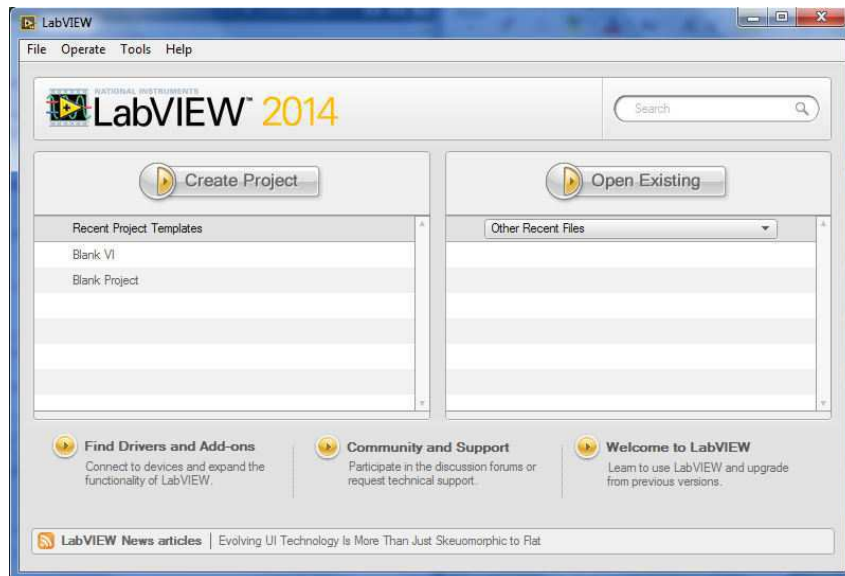


Figure 3.15: labview creating project

which 6 can be used as PWM outputs and 6 can be used as analog inputs). It has quartz crystal, a USB connection, a power jack, an ICSP header and a reset button, and presents a maximum DAQ rate of 10

<b>Microcontroller</b>	<b>ATmega328</b>
<b>Operating Voltage</b>	<b>5V</b>
<b>Input Voltage (recommended)</b>	<b>7-12V</b>
<b>Input Voltage (limits)</b>	<b>6-20V</b>
<b>Digital I/O Pins</b>	<b>14 (of which 6 provide PWM output)</b>
<b>Analog Input Pins</b>	<b>6</b>
<b>DC Current per I/O Pin</b>	<b>40mA</b>
<b>DC Current for 3.3V Pin</b>	<b>50mA</b>
<b>Flash Memory</b>	<b>32KB (ATmega328) of which 0.5 KB used by bootloader</b>
<b>SRAM</b>	<b>2KB (ATmega328)</b>
<b>EEPROM</b>	<b>1KB (ATmega328)</b>
<b>Clock Speed</b>	<b>16MHz</b>

Figure 3.16: Technical specification of the Arduino UNO R3 board [42]

**NI-6002 board +labview** : The USB-6002 is a low-cost, Full speed USB, multi-function DAQ (Data acquisition) device. It offers eight single-ended analog input (AI) channels, which may also be configured as four differential channels. It also includes two analog output (AO) channels, 13 digital input/output (DIO) channels, and a 32-bit counter. The USB-6002 provides basic functionality for applications such as simple data logging, portable measurements, and academic lab experiments. Other characteristics important to know are enumerated in the table in Figure 3.17

Feature	NI USB-6002
<b>Analog input</b>	
Analog-to-digital converter (ADC) Resolution	16-bit
Maximum Sample Rate (aggregate)	50 kS/s
<b>Analog output</b>	
DAC Resolution	16-bit
Absolute Accuracy, Typical, at full scale	8.6 mV

Figure 3.17: technical specification of NI USB-6002 (datasheet)

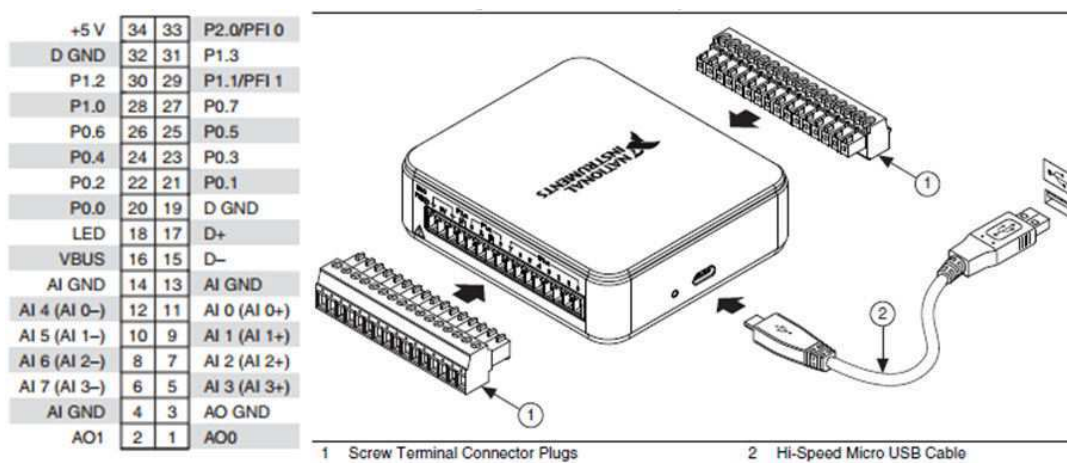


Figure 3.18: NI-USB 6002 Pin guide [43]

### 3.3.9.2 Accuracy Test

In order to test accuracy. A constant voltage divider output is run into the analog input pin of the board. The appropriate IDE for each board is then used to visualize the input signal. Figure 3.19

**Arduino UNO** : Arduino UNO is equipped with a 10 bit Analog-to-digital converter. This means that it will map input voltages between 0 and  $V_{ref}$  into integer values between 0 and 1023. (Resolution =  $V_{ref} / 1024$ ) Input range and resolution can be changed using *analogReference()*. The options for the reference voltage are:

- **DEFAULT**: the default analog reference  $\approx 5$  volts and comes from the main power supply of the Arduino board which is through USB.
- **INTERNAL**: an built-in reference, equal to 1.1 volts since It comes with ATmega328 microcontroller.

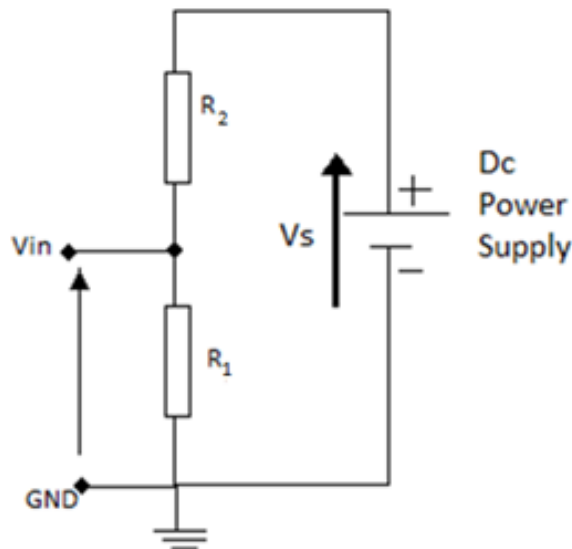


Figure 3.19: basic circuit for accuracy tests

- **EXTERNAL:** the voltage applied to the AREF pin (0 to 5V only) is used as the reference.

ADC readings are visualized using a terminal interface of the Arduino development IDE

**Part One** :These tests are to study the effect of the reference voltage mode on the reading stability.

**First Test(Default Aref):** we set  $R_1 = R_2 = 470K\Omega$ , and  $V_{ref}$  is set to default.  
code:

```
// the setup routine runs once when you press reset:
void setup() {
  // initialize serial communication at 9600 bits per second:
  Serial.begin(9600);
}
int sensorValue;
int i;
// the loop routine runs over and over again forever:
void loop() {
  // read the input on analog pin 0:
  for(i=0;i<20;i++)
  {sensorValue = analogRead(A0);
  // Convert the analog reading (which goes from 0 - 1023) to a voltage (0 - 5V):
  // print out the value you read:
  Serial.print(' ');
  Serial.print(sensorValue);}
  delay(3000);
  Serial.println();
}
```

Figure 3.20: Reading analog voltage -arduino code

and by using the IDE terminal we obtain:

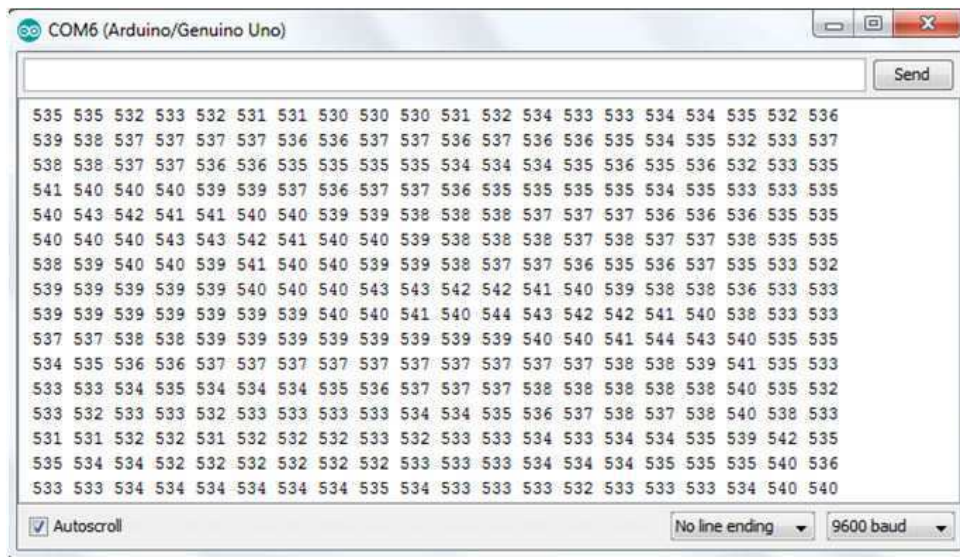


Figure 3.21: Reading analog voltage-arduino IDE

*Observation:* from Figure 3.21 we see Fluctuations that go up to 7-8 bits.

**Second Test(External Aref):** A 5V DC power supply is connected to Aref pin. A protective  $1K\omega$  resistor is used for when another mode is activated while an external DC supply is still connected to Aref pin. ( $1k \ll 100k$  which is the input impedance of the analog pin. [44])

The same code is used except that the instruction analog reference(EXTERNAL) is added to the setup part.

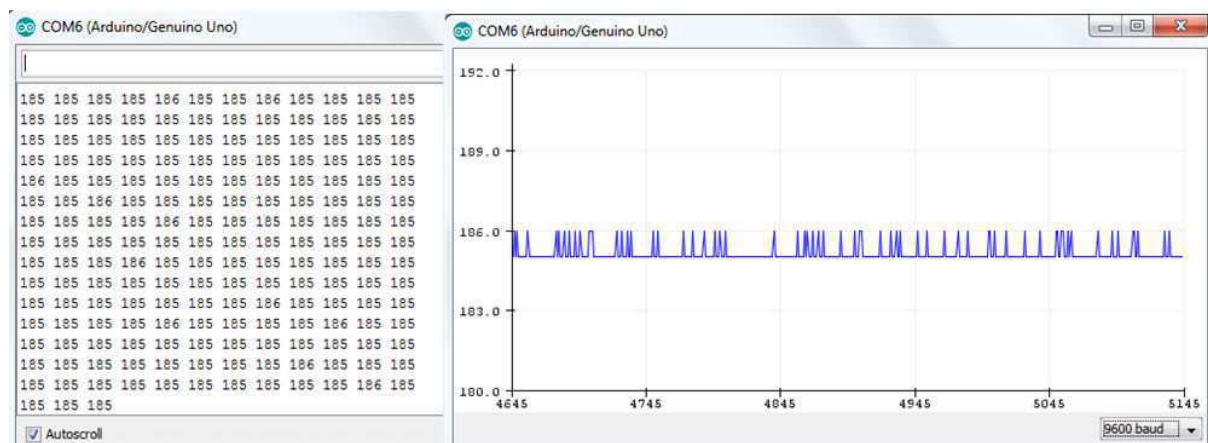


Figure 3.22: Analog read with External Aref

**Third Test(Internal):**Resistors from the previous test are replaced such that the measured voltage does not exceed  $V_{ref}$ . This latter is in this case provided directly by the microcontroller and is much more steady than the DEFAULT ref with a value of 1.1v Figure 3.23

*Code:* we use the same code except the instruction Analog-reference is replaced by by Analog-reference(EXTERNAL).

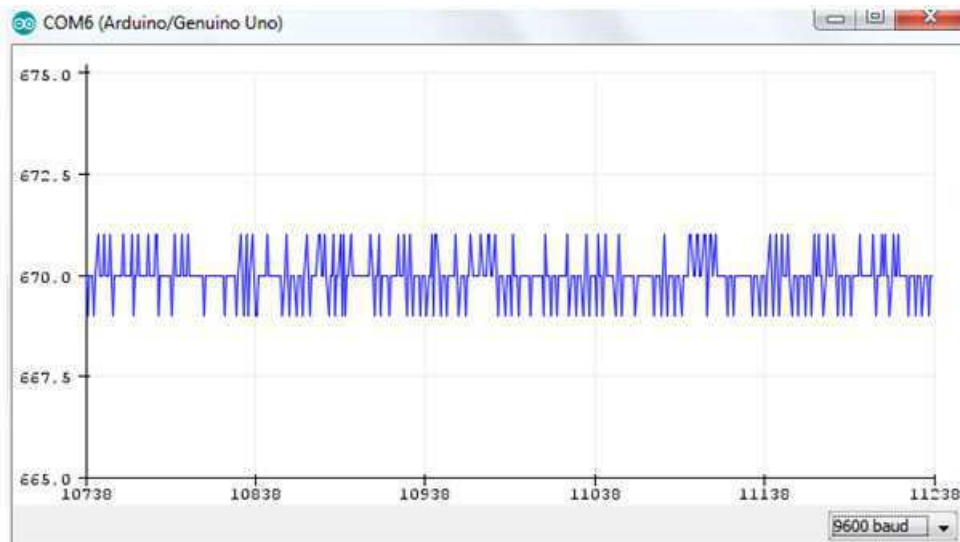


Figure 3.23: reading with External Aref

*Observation:* Stabilizing the Reference voltage does stabilize the analog readings. However with an internal reference of 1.1 V sensitivity is reduced (input range is too small)

**PART Two: First test** in this part  $R_1$  and  $R_2$  are replaced respectively by one FSR element and a  $9M\Omega$  resistor. Figure 3.24

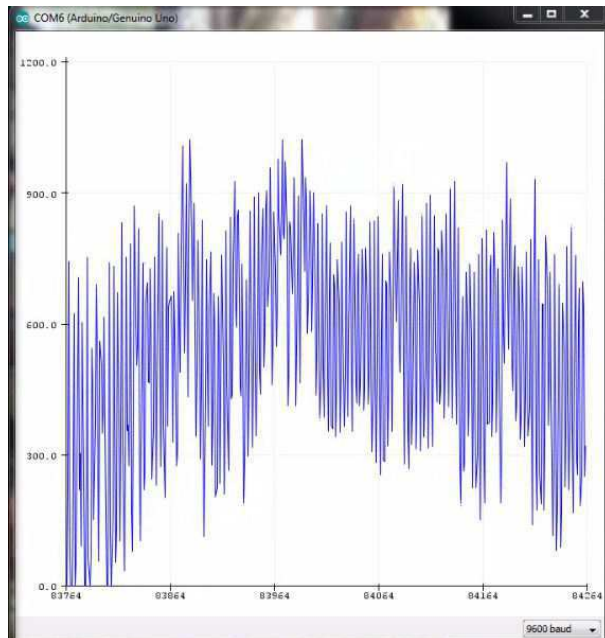


Figure 3.24: FSR element test

*Observation:* Fluctuations that go up to 20 bins i.e. Error = 100 mV. For a set of 3 variable error estimated for one FSR exceed  $1M\Omega$ ! Same phenomenon was observed in DEFAULT and INTERNAL mode.

**Conclusion:** The ADC accuracy does also have to do with ZO (see the diagram above).

**Explanation:** This relation between accuracy and  $Z_o$  is the fact that the analog pin inner circuitry comprises a sample and hold block followed by the ADC. The sample and hold part guarantees a constant input value for the ADC while it proceeds with the conversion and its equivalent circuit is represented in Figure 3.25

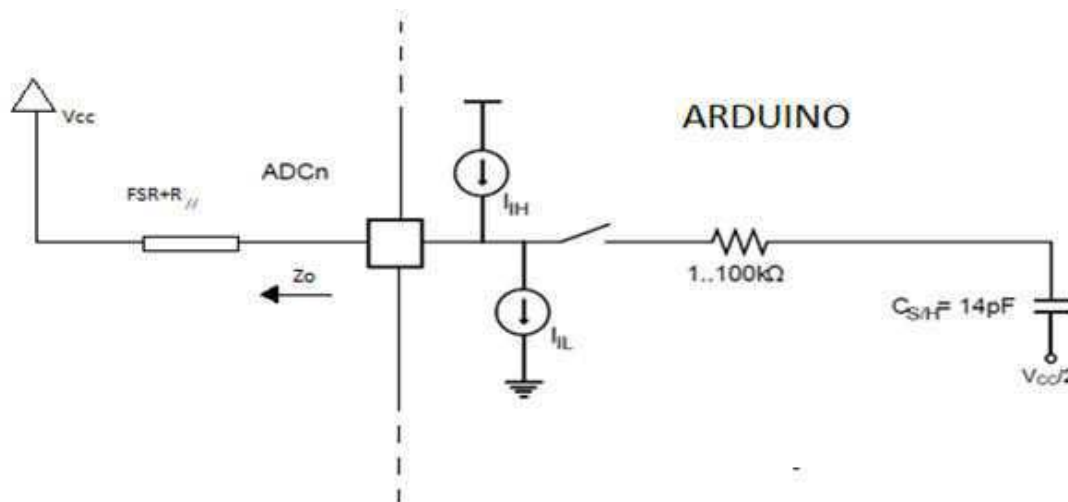


Figure 3.25: Sample and hold-arduino board

It can easily be seen that if  $Z_o$  is too high, the capacitor  $C_{s/h}$  will take too long to charge, hence the fluctuations. Matter of fact, it is recommended to use  $Z_o < 10$  k. [44] One solution is to place a buffer before the analog pin (Figure 3.26 reduces the charging time of  $C_{s/h}$ . Results similar to those in PART One are obtained.

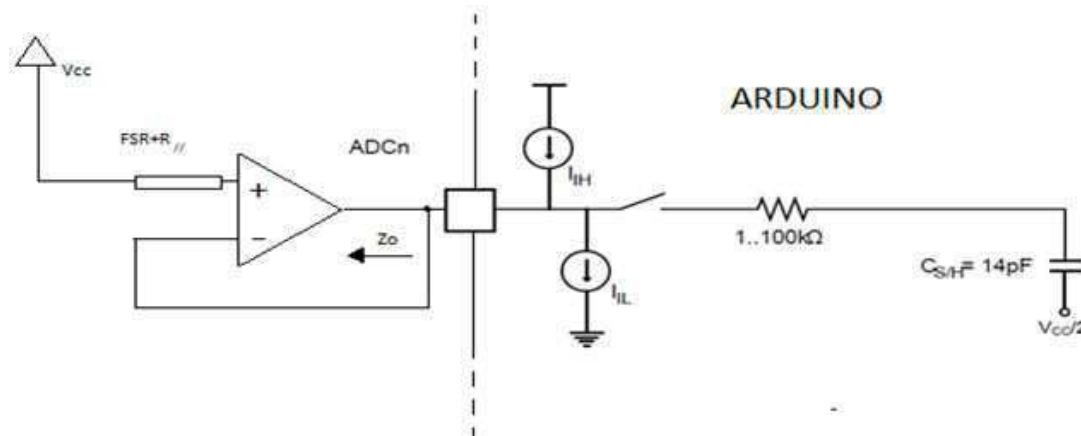


Figure 3.26: Analog read using buffers

#### NI-USB 6002 :

Some interesting characteristics indicated by its datasheet include:

- It presents a bigger range which allows us to amplify the input voltage as to reduce the effect of noise that generated by the card's circuitry on the measurement.
- Unlike the Arduino the Analog reference voltage is always set to a default value of 10 V. We cannot control it.

- It also presents a full scale error of 8,6 mV.

**Tests:** Two tests were run in order to study error due to high impedance measurements. we set the power supply  $V_s$  to 9v

1.  $R_1 = R_2 \approx 470K\Omega$ . the output impedance is equal to  $Z_o = 235K\Omega$ . we observe a fluctuation of 9mV which is equivalent to about 2 bins in arduino ADC
2.  $R_1 = 9M\Omega, R_2 \approx FSR$ , fluctuation is increased.

Fluctuations are high for high impedance values but are less than the ones recorded by Arduino. It can clearly be seen that this board presents a higher dynamicity. Similarly, a buffer can be used in order to eliminate the high impedance effect on the reading accuracy.

### 3.3.9.3 Comparison

The two boards present approximately the same error with NI USB-6002 being more dynamic with high frequencies.

*Data acquisition rate:* Analog read takes about 100 microseconds (0.0001 s) (maximum acquisition rate of 10 KHz). This is about 5 times slower than the NI board. Furthermore, the ADC resolution is better in Ni boards than in Arduino UNO boards. NI-6002 comprises a faster system clock.

## Conclusion

This chapter was to design the system which will consist of a pressure mat built from copper adhesive and sensor film kit, the conditioning circuit which is for selecting the FSR to measure, amplifying the voltage to measure and "isolating" the activation voltage. The role of each component is clarified, and a NI USB-6002 board which was selected for data acquisition which will be combined with a suitable labview interface.

The next chapter is to deal with implementations, of both hardware and software of the system.



## CHAPTER 4

# Chapter 4

## Implementation, Calibration and Final Tests

After design comes execution. This chapter describes the implementation process of both hardware and software of the prototype. It also includes the calibration outcome and deficiencies and last but not least, tests of the resulting system's specification.

### 4.1 Calibration

#### 4.1.1 What makes a good sensor

The three most important characteristics of a sensor in our case are:

1. **precision:** An ideal sensor always produces the same output for the same input and that means immunity against:
  - (a) *Noise:* In our case there will be noise due to the full scale error of NI board. Furthermore, all measurement systems are subject to random noise to some degree and that includes ground loops, connectivity issues, etc.
  - (b) *hysteresis:* Some types of sensors also exhibit hysteresis. The sensor will tend to read low values with an increasing signal and higher values with a decreasing signal. Hysteresis is a common problem with many pressure sensors.
2. *Resolution:* The smallest change a sensor can detect.
3. *speed:* Precise reading regardless if the speed at which varies the measurand.
4. *Linearity* is also a good thing to have but in our case we will just have to be content with what piezoresistive material offers.

### 4.1.2 Calibration technique

There are numerous techniques used for calibrating pressure sensors. See section 2.3. In our case, we are simply measuring the resistance of a given surface  $S = 10\text{cm} \times 8\text{cm}$  of the piezoresistive film when a load of a given weight  $W$  is applied to it. For a homogeneous force distribution a rigid plate (preferably metal but we used wood) of a same size is the calibrated element. Resistance is measured using a simple voltage divider circuit.



Figure 4.1: Calibration of FSR

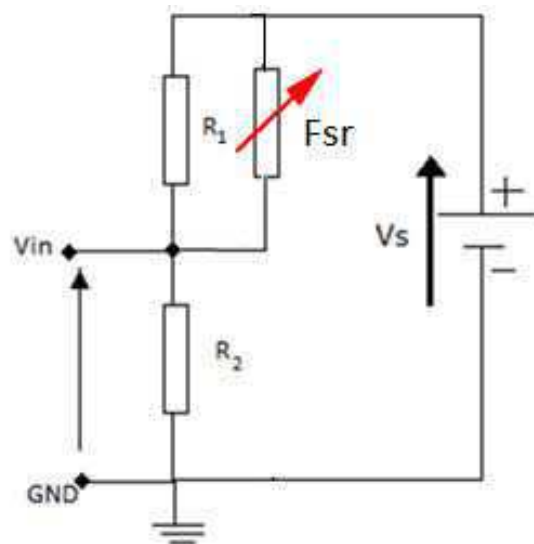


Figure 4.2: testing circuitry

The experimental measured values of  $V_s$ ,  $R_1$  and  $R_2$  are respectively 9.72 V , 252  $K\Omega$  and 256  $K\Omega$ . Note that the FSR film is connected in parallel with a much smaller resistance. This is to omit the measurement fluctuations that are due to the influence of high impedance on the multimeter.

- A range of 100 g to 3.5 Kg of load is applied.
- If we suppose that the sensing film is homogeneous, resistance of the little FSR elements is deduced based on equation 2.1.
- $R$  is calculated based on the following formula:

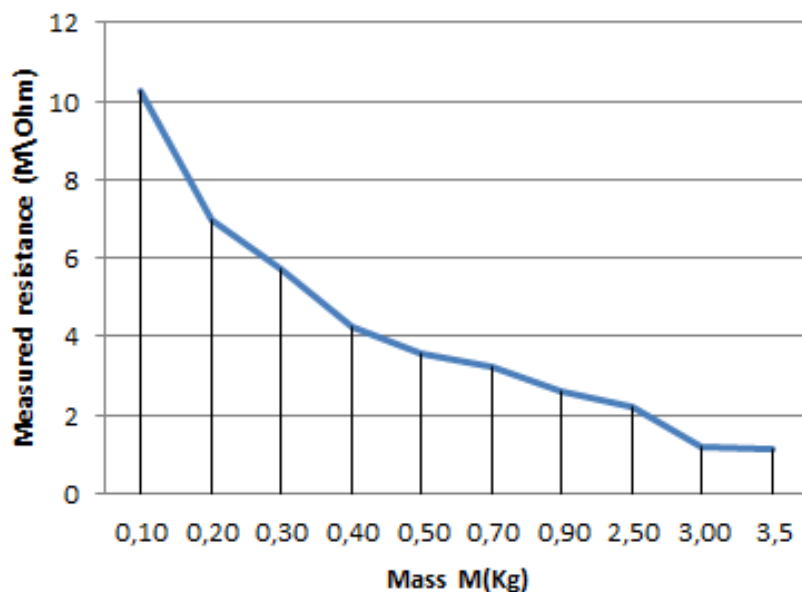
$$V_{in} = \frac{R_2}{R_1 \parallel f_{sr} + R_2} V_s \Rightarrow f_{sr} = \frac{R_2 * R_1 * (V_s - V_{in})}{(R_1 + R_2) * V_{in} - R_2 * V_s} \quad (4.1)$$

-**Observation:**Fluctuations of up to 0.5V in the measured voltage which makes it impossible to evaluate hysteresis and also to obtain an absolute pressure-resistance graph.To analyze the problem  $V_{in}$  is measured while Fsr is disconnected: A significant reduction in fluctuation is observed.

-**Conclusion:**Response of the sensing film does not stabilize in the very limited time span.However several values were recorded and a mean value  $V_m$  was taken for each input.

Mass ( kg)	0,1	0,2	0,3	0,4	0,5	1	1,5	2,5	3	3,5
$V_m$	4.94	5.01	5.03	5.07	5.1	5.12	5.17	5.22	5.5	5.55
$R_m (M\Omega)$	29,077	6,947	5,725	4,247	3,566	3,225	2,609	2,198	1,2	1,115

Figure 4.3: table of calibrated FSR



Note: pressure is  $\frac{F}{A}$ . Where A is the area of the sensing element and F is the ground reaction force which, on a horizontal plane is equal to the gravitational force acting upon the subject. In this graph resistance is expressed in terms of mass but the pace is the same for pressure. (the gravitational acceleration is the same and the surface of the film is the same)

**Calibration for load in the order of human weight:** This is done using a good quality scale to which the FSR film along with the wooden plate are mounted. The scale is used to measure the weight of the subject as he/ she they stand on the FSR film. This latter is mounted into the same voltage divider circuit to measure the value of resistance. An alternative method was used due to time and material shortage circumstances : The calibration graph was drawn based on that provided by the fabricator of the material. (See Figure 4.4) It can be seen that the variation of resistance is of an inverted exponential pace.  $\Rightarrow$  Our sensors are not linear.

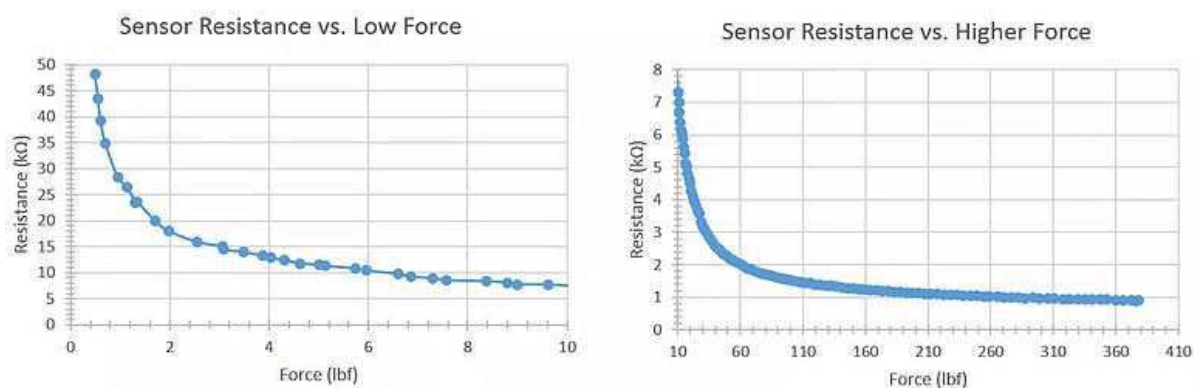


Figure 4.4: calibration of the force sensor by the fabricator

An “exponential “ extrapolation of the previous measurements can be used.

**conclusions** Taking into account the response of the sensing film, and until further studies of the material, it can be said that it is mostly adequate for binary sensing(detection). Note that this project still includes calculation of the values of the resistors based on the collected voltages. For now, the corresponding pressure values are to be taken from graphs presented above for mere proof of concept. The real pressure values are bound to either further studies or other calibrations circuits that might reduce noise which will be undertaken in future complementary works. Note: Dynamic calibration cannot be done for inaccessibility to the necessary material.

## 4.2 Implementation

### 4.2.1 The pressure mat

This section describes the implementation of the mat as described in detail in section 2.2

1. A gerflex flooring shown in Figure 4.5 is used as the base material. It is the base layer of the mat on which it is practical to trace paths of the upper layer strips and emplacements of the pressure sensing squares.



Figure 4.5: (a)Mat construction

2. On the top of flooring layer, a set of 28 1.78m long copper stripes are set parallel to one another and spaced by 1.4cm. The conductive side of the copper is to come in contact with the piezoresistive film squares. This copper tape from **Sparkfun** is 5 mm wide and comes with a conductive adhesive back.
3. deposit of 0.7cm X 0.7 cm FSR square elements which are spaced by 1.4 cm horizontally and 1.7 vertically (this defines the dimensions of a single sensel i.e. sensing unit)
4. A set of 105 parallel copper strips are set orthogonally to the bottom copper layer as to form a matrix as shown in Figure 4.6  
The copper strips are spaced by 1.7 cm and set such that each sensing elements is at an intersection of two stripes from opposite layers.



Figure 4.6: (b)Mat construction

5. Connectors are welded to their respected rows and column
6. The mat is covered by a protective cellophane sheet.

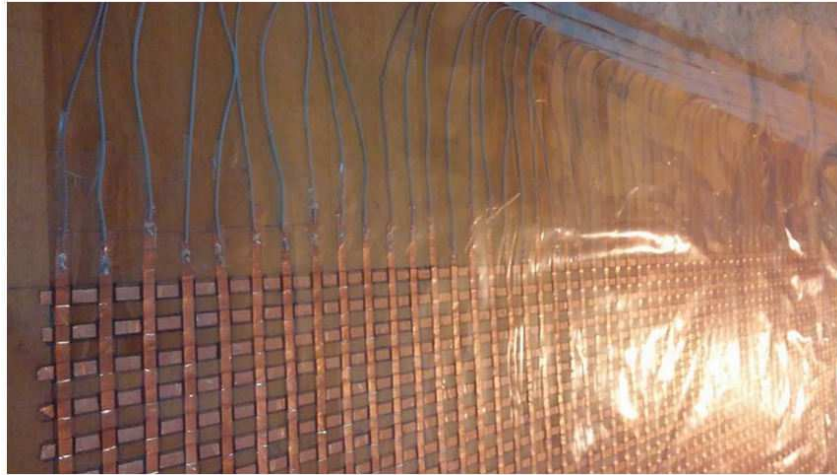


Figure 4.7: Final Result

## 4.2.2 Conditioning circuitry

After the simulation and validation of different part of the system and of the system as a whole (see chapter 3). A printed circuit board is implemented based on the same model, using Proteus 8.4 Professional which includes a dedicated layout software.

### 4.2.2.1 Schematic capture

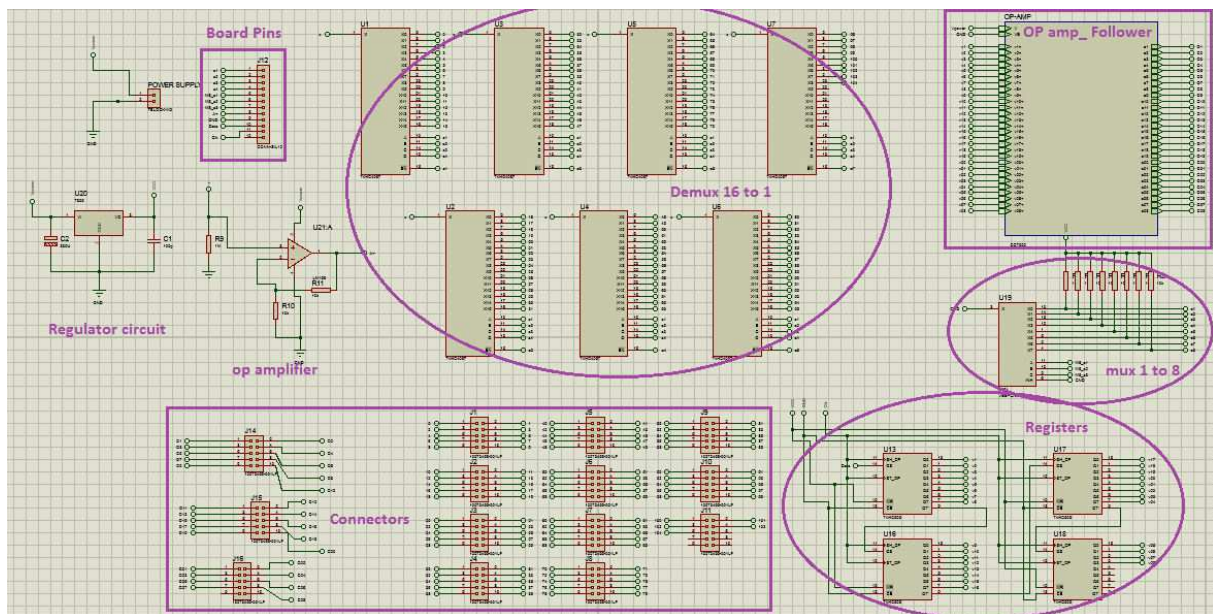


Figure 4.8: Schematic capture

Note that amplifying stage was added the circuit to amplify the voltage that goes into the analog pin of the board and that is by a gain = 2. Two 10 K resistors were used along with a LM158j dual operational amplifier

The powerl supply bloc consist of a DC stabilized power supply that ouputs a voltage of 12 V. The 12 V rails is connected to the V+ pin of the Op amps and the input of the

5V regulator. The 5V rail (5V is generated by the regulator. Is connected to Vcc pins of Multiplexers and registers.

#### 4.2.2.2 Routing

Before launching the auto-route tool. The following PCB parameters Design Rule Manager are set, with trace = 0.03in :

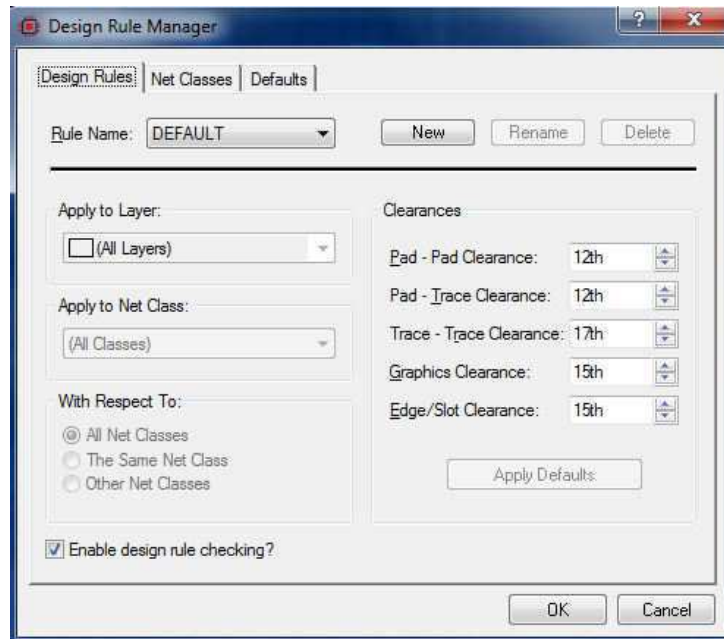


Figure 4.9: Design Rule Manager

Next, Signal traces are routed. As it appears that it is not possible to fit all the wire into one side of the board. A double sided PCB layout is created :

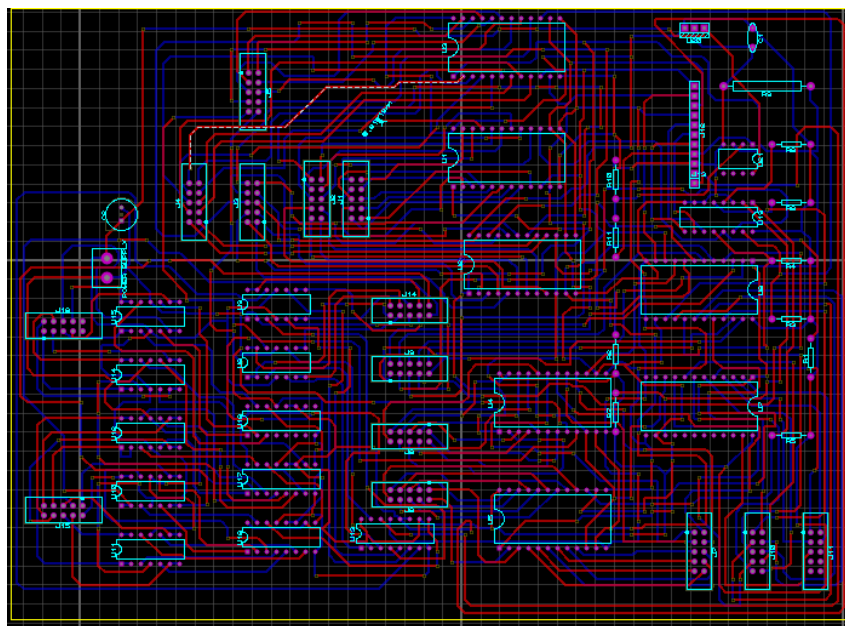


Figure 4.10: Printed circuit with two side



A final step is to mount the components into the printed circuit board and check for continuity in connections.



Figure 4.11: Printed circuit with two side

## 4.3 Software application

### 4.3.1 General description of the interface

A 14.0F1 version of LABVIEW is used to implement a graphical user interface Which serves to visualize the subject's gait through two types of profiles:

- *A real time binary plantar profile* : Foot steps are traced in white on a black background as the subject walks on the mat. It is basically a binary pressure image where if a sensor is pressed, the collected voltage exceeds the threshold value and the corresponding pixel value is switched to on. Information drawn from this kind of images are limited and related only to people or object displacements on the pressure platform.

- *A grey- level plantar profile (colored)* : Each pixels value is a function of pressure that is applied to the corresponding sensors. Grey-level images are characterized by a higher information content. Pressure images are generated after the real value of FSRs are calculated *regardless of the quality of the measurement*.

Due to the limited specification of the acquisition system (a rate of 50 kHz instead of a least required of 358.6 KHz), it is preferable to calculate the real values of the platform FSRs after the real time visualization which is stopped by clicking on the stop button.

### 4.3.2 Block diagram

this schema block present the total program

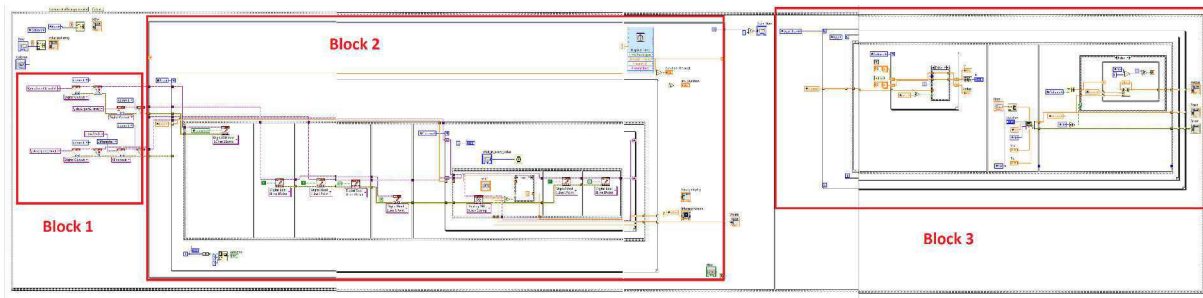
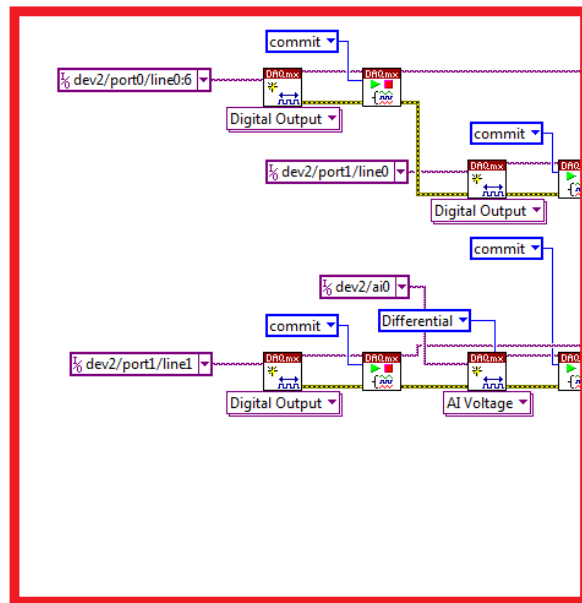


Figure 4.12: LabView Block diagram



## Block 1

Figure 4.13: Block 1

### Block 1:

It contains analog and digital pin monitoring modules:

- Analog input (AI) DAQ assistance modules** : *Read vi*. Set to Analog input voltage (AI), allow us to select a physical channel for the task through which data is acquired and configure the selected terminal's mode : differential or RSE. In RSE mode, input is measured relative to the ground rail of the board which is set by the USB power unit. In differential mode the input voltage is measured using two "coupled" pins. Each of these pins is connected to one terminal of the dipole across which voltage is measured. Each analog pin is associated with another analog pin in case of differential functioning. Differential mode is generally used to eliminate ground loops.
- Modules start and stop task VI** are used to start task prior to the for loop and stop it after the for loop , instead of starting and stopping it repeatedly at the execution of each iteration. This improves the performance of the scanning process.

Ni-6002 I/O pin	component pin
port0/line0	s1 (16to1 Demux inputs)
port0/line1	s2 (16to1 Demux inputs)
port0/line2	s3 (16to1 Demux inputs)
port0/line3	s4 (16to1 Demux inputs)
port0/line4	1to8 MUX S1 input( $M8 - S1$ )
port0/line5	1to8 MUX S2 input( $M8 - S2$ )
port0/line6	1to8 MUX S3 ( $M8 - S3$ )
port1/line0	Register Data pin
port1/line1	Register Clk pin
AI 0+	Ao pin of LM324 op-amp
AI 4-	GND

Table 4.1: NI 6002 pin redirection

Task vi allows us to eliminate a set of procedures that are run when reading , or writing to analog to digital pin.

- **The modules with the digital output indication** are used to write Boolean value(s) to one or more physical channels that are specified in task.

**Block 2 :**

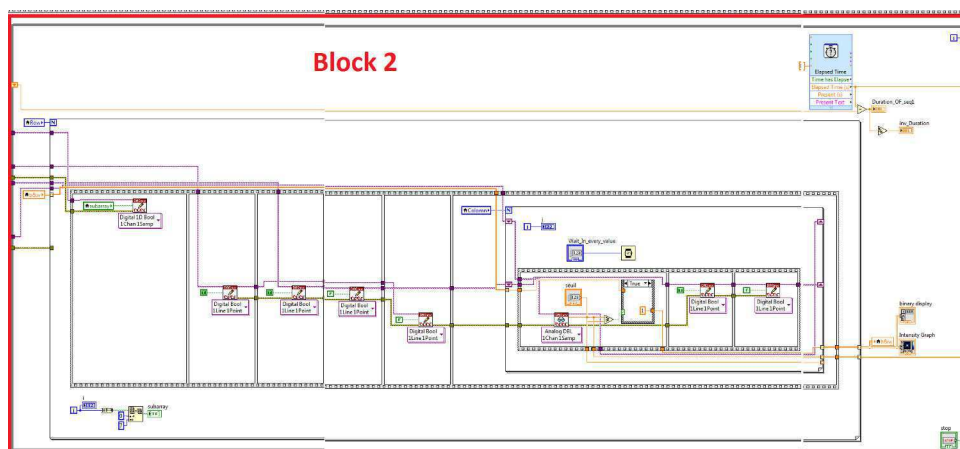


Figure 4.14: Block 2

It executes the following operations: **Scanning the pressure platform:** just as described in section 3.2 the program begins the scan of each row by:

- selecting the row of index  $i$  by setting the lines 0-7 the binary value of the index  $i$ . This means that the digital output are to monitor the selecting pins of the multiplexers as to select row of index ( $i$ ). Table 4.1 indicates which line correspond to which pin on the PCB.
- generating an impulse that goes into the first register's serial input. This is done by setting the data pin (port1 line 0) to "high" value (which is 5v) and that is for a duration of one clock high state.

Once a row is selected and an impulse is generated and driven into the first column, another FOR loop is launched where each iteration corresponds to a certain column and for each column data is acquired (AI activated) then processed and then the activating impulse is shift to another column and that is by sending a clock impulse into the common clock pin of the shift registers which is connected to (port1, line1) Data processing for this block contains comparison to a threshold voltage followed by:

1. Setting the value of the corresponding element in another binary matrix B and W to 1 if the pressure cell is pressed. Thereby, this allows us to generate a 105x28 binary matrix that will be driven into a graph chart which results in the binary level pressure image.
2. Selecting the voltage values that exceeds the threshold and saving them in a matrix for when the subject finishes walking and data acquisition is stopped. Meanwhile a While loop is for scanning the mat over and over.

**Block 3 :**

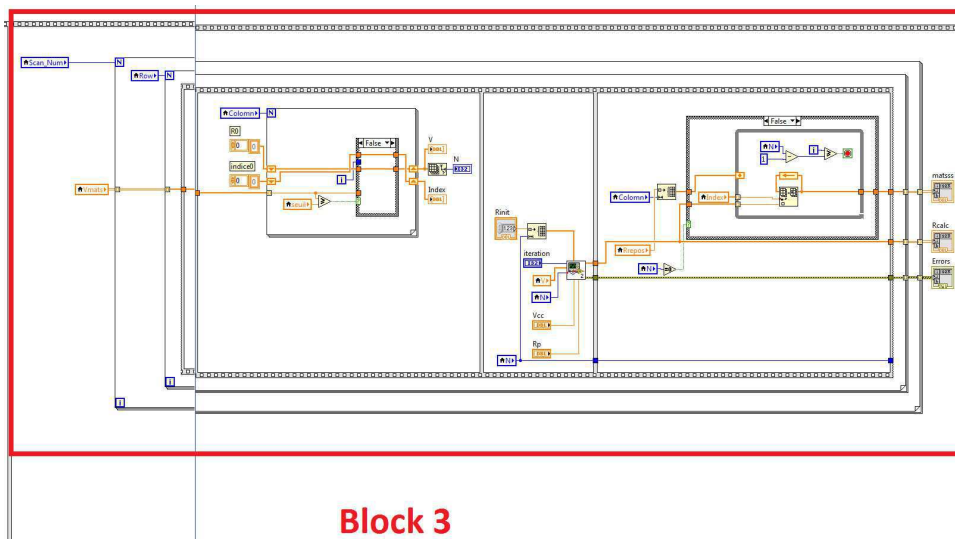


Figure 4.15: Block 3

this block is activated once the STOP button is pressed It collects data derived by Block2 and which consist of 3D matrix and that is a series of 2D matrix included one 3D matrix. Each matrix contains voltages value from one single sweep of the mat that are above the threshold. This block uses a couple of matlab modules to calculate the values of the corresponding resistors. These values are then inserted back into a new matrix row by row. The column index is taken from block 2.

**Matlab scripts**Figure 4.16 The first matlab block generates the formula expressing  $R_{i+1}$  in terms of R1 based on the number of variables. Other parameters are : Vcc value (Just in case shift register doesn't deliver 5V) , Rp value (which is 1Mohms). The second Matlab value uses the formula generated by the first block and calculates the the solution of the equation set departing from a given value of Rp that is chosen in a way that the method converges. (see appendix C)

Note : Due to time limitations .This application is designed for essential demonstrations.The generated results can be used to calculate more spatial and temporal parameters and more modules can be added into the interface

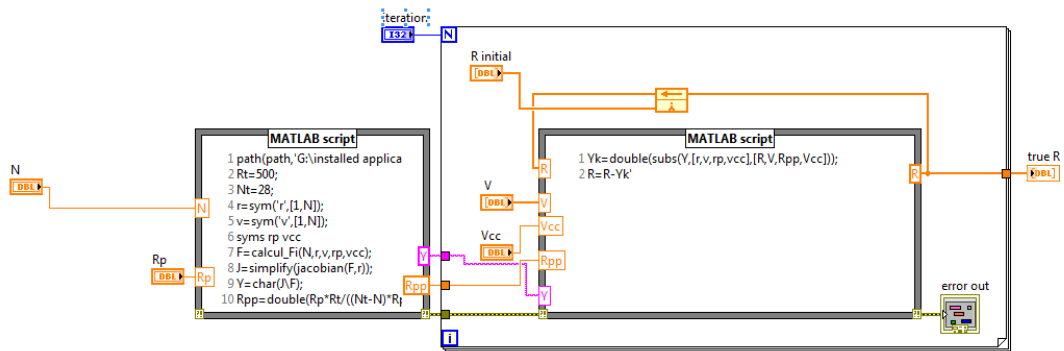


Figure 4.16: Matlab SubVi

```

1  function F=calcul_Fi(N,r,v,rp,vcc)
2  %this function generate Fi formula
3  F=1;
4  for j=1:N
5  Req=rp;
6  for i=1:N
7      if i==j
8          continue;
9      end
10     Req=Req*r(i)/(Req+r(i));
11     Req=simplify(Req);
12 end
13 f= Req*vcc/(Req+r(j))-v(j);
14 f= simplify(f);
15 F=[F;f];
16 end
17 F=F(2:N+1,1);
18 end

```

Figure 4.17: code MatLab

## 4.4 Final Tests

The first test is to check for continuity of the pads in the circuit and connect two equivalent points that are on different sides of the board. This later is then connected through the circuit. A stabilized 10 V DC source is used at the entrance of the regulator. The Following tests included testing in-site of components individually. Next, readings were recorded using both Analog read and a multimeter.

## Results and conclusions

1. The scanning process is operative
2. For one selected FSR, the collected voltage depends on only FSRs from the same matrix.
3. Unladen operation: Voltage collected for different FSR on which no load was applied differs from one FSR to another and proved to be higher than expected.  $\Rightarrow$  Detection is not possible but it is still possible to calculate the values of FSRs that are from the same row.

## Explanation

- Lack of part to part repeatability: It has proved to be impossible to obtain 2940 sensing elements that are 100% identical. This resulted in a difference in resistance values between FSRs across the mat which explain the difference in readings.
- The unexpected voltage collected for a non pressed sensel shows that this sensel is pressed after all. This pressure comes from the upper layer copper strips. These strips exert a certain pressure on the FSRs as they fasten them to the flooring.
- pressure exerted by the copper strips is enough for the sensing material to enter the low sensitivity range.

## Solution

- A first solution is an automated fabrication process which ensure part to part repeatability. Spacers can be added to keep the sensing element.
- Another solution is to find another sensing material with lower impact strength (it has to remain elastic though) and an adequate load range.

# General Conclusion

First, Although the system is not operative yet, this project has been of a great interest as it allowed us to concertize skills we have acquired during the past five years and use them in a very interesting application.

Second, This thesis introduced us to the domain of gait analysis which is of key importance in many applications of which we encountered many effective research examples. We were captured by the major attention it has drawn in the last years and which resulted in the development of various technologies that are based on simple, yet very helpful ideas. We learned about the techniques that are used in such technologies, the pros and cons of each type and the challenges encountered in the realm of gait tool instrumentation.

Automatization is a must when it comes to building large platforms. The limited access to adequate fabrication and calibration procedure has made access to the utility of the mat less than possible. However it can be said that it give possibilities to some interesting projects and future complementary works that are based on the same technology but on a smaller scale platorm where work on the algorithmic scale as well as signal processing can be done. For instance, algorithms for calssification can be implemented eitherby traditional methods like matlab or neuronnes networks.

We also expect to lead a more thorough study of the sensing film which proved to be inconvenient for Our application and probably find other alternative materials, or platform strucutres. A study can also be lead IP systems, and other kinds of gait analysis systems. *This is just the beginning of a long journey!*

# Bibliography

- [1] Alvaro Muro-de-la-Herran, Begonya Garcia-Zapiran, and Amaia Mendez-Zorrilla. “Gait Analysis Methods: An Overview of Wearable and Non-Wearable Systems, Highlighting Clinical Applications”. In: *Sensors* 14 (2014), pp. 3362–3394.
- [2] Kharb Ashutosh, Saini Vipin, and Surender Dhiman Y.K Jain. “A REVIEW OF GAIT CYCLE AND ITS PARAMETERS”. In: *IJCEM International Journal of Computational Engineering and Management* 13 (july,2011).
- [3] R. GAGE JAMES, A. DELUCA PETER, and THOMAS S. RENSHAW. “Gait Analysis: Principles and Applications”. In: *The Journal of Bone and Joint Surgery* 77 (1995), pp. 1607–1623.
- [4] Ross Bogey. *Gait Analysis*. Aug. 2016. URL: [Link](#).
- [5] Pachi, Aikaterini, and Tanjian. “Frequency and velocity of people walking”. In: *The Structural Engineer* 83 (2005).
- [6] J.Afilalo et al. “Gait speed as an incremental predictor of mortality and major morbidity in elderly patients undergoing cardiac surgery”. In: *US National Library of Medicine National Intitute of Health* (Nov. 2010).
- [7] Sally Moore et al. “Observation and analysis of hemiplegic gait:swing phase”. In: *Australian Physiotherapy* 39.4 (1993).
- [8] BHAVE ANIL, PALEY DROR, and E. HERZENBERG JOHN. “Improvement in Gait Parameters After Lengthening for the Treatment of Limb-Length Discrepancy”. In: *The Journal of Bone and Joint Surgery* (1999).
- [9] Michael W Whittle. “Gait Analysis an Introduction”. In: chap. *Methods Of Gait Analysis*.
- [10] P. Heckmann Timothy, Frank R. Noyes, and Sue D. Barber-Westin. “Correction of Hyperextension Gait Abnormalities: Preoperative and Postoperative Techniques”. In: ().
- [11] Stanford Medicine 25. *Gait Abnormalities*. 2015. URL: [Link](#).
- [12] Lara Allet et al. “Wearable Systems for Monitoring Mobility-Related Activities in Chronic Disease: A Systematic Review”. In: *Sensors* 10 (2012), pp. 9026–9052.
- [13] Sam Patel et al. “A review of wearable sensors and systems with application in rehabilitation”. In: *Journal of Neuroengineering and Rehabilitation* 9.21 (2012).
- [14] Joonbum Bae and Masayoshi Tomizuka. “A tele-monitoring system for gait rehabilitation with an inertial measurement unit and a shoe-type ground reaction force sensor”. In: *Mechatronics* 23 (2013).
- [15] Crea S, Derossi, and DONati. “A Wireless Flexible Sensorized Insole for Gait Analysis”. In: *Sensors* 14 (2014).



- [16] Matej Andrejašic. *MEMS ACCELEROMETERS. Seminar*. 2008.
- [17] Ibrahim AlMohimeed. “Development of Wearable Ultrasonic Sensors for Monitoring Muscle Contraction”. MA thesis. Ottawa-Carleton Institute for Biomedical Engineering, 2013.
- [18] *Human Gait Recognition using Silhouette Vector and Principal Component Analysis*. 1. IJCA Journal, 2014.
- [19] Rod Cross. “Standing, walking, running, and jumping on a force plate”. In: *American Association of Physics Teachers* 67.4 (Apr. 1999), pp. 304–309.
- [20] Robert J. Orr and Gregory D. Abowd. “The Smart Floor: A Mechanism for Natural User Identification and Tracking”. In: *Short talks* (2000).
- [21] MICHAEL D. ADDLESEE et al. “The ORL Activ Floor”. In: *IEEE personal communication* (2000).
- [22] Ryan Rainone, Benjamin Gardner, and Jonathan Frost. “Gait Efficiency Analysis Using Three Axis Force Plate”. PhD thesis. Faculty of WORCESTER POLYTECHNIC INSTITUTE, Apr. 2008.
- [23] Maarten Oosterlinck et al. “Comparison of pressure plate and force plate gait kinetics in sound Warmbloods at walk and trot”. In: *The Veterinary Journal* (2009).
- [24] Martino Lombardi, Vezzani Roberto, and Rita Cucchiara. *Detection of Human Movements with Pressure Floor Sensors*. Tech. rep. Softech-ICT University of Modena and Reggio Emilia- Modena-Italy.
- [25] *Force sensing resistor theory and application*. Sensitronics.
- [26] F Mokhtari, M Latifi, and M Shamshirsaz. “Electrospinning/electrospray of polyvinylidene fluoride (PVDF): piezoelectric nanofibers”. In: *The Journal of The Textile Institute* (2015), pp. 1–18.
- [27] Stephen Urry. “Plantar pressure-measurement sensors”. In: *Measurement Science and Technology* 10 (1999), R16–R32.
- [28] Abdul Hadi Abdul Razak et al. “Foot Pressure Measurement System A REVIEW”. In: *Sensors* (July 2012), pp. 9885–9912.
- [29] Holger Böse, Eric Fub, and Philipp Lux. “Influence of Design and Material Properties on the Performance of Dielectric Elastomer Compression Sensors”. In: *Electroactive Polymer Actuators and Devices*. Ed. by Yoseph Bar-Cochan. Vol. 9430. 943029. Proc. of SPIE, 2015.
- [30] Holger Böse and Eric Fub. “Novel Dielectric Elastomer Sensors for Compression Load Detection”. In:
- [31] *FBG - FIBER BRAGG GRATING PRINCIPLE*. URL: [Link](#).
- [32] *Fundamentals of Fiber Bragg Grating (FBG) Optical Sensing*. Jan. 2016. URL: [Link](#).
- [33] Ebrahim Al-Fakih, Noor Azuan Abu Osman, and Faisal Rafiq Mohamd Adikan. “The Use of Fiber Bragg Grating Sensors in Biomechanics and Rehabilitation Applications: The State-of-the-Art and Ongoing Research Topics”. In: *Sensors* 12.10 (2012), pp. 12890–12926. URL: [Link](#).
- [34] Wei-Chih Wang et al. “A Shear and Plantar Pressure Sensor Based on Fiber-Optic Bend Loss”. In: *JRRD* 42.3 (May 2005), pp. 215–326.

- [35] Chavez Pirson. “The Basics of Fiber Bragg Gratings”. In: *SENSOR TECHNOLOGY AND DESIGN* (Aug. 2004). URL: [Link](#).
- [36] Tae-Sung Lee, Yong-Moo Kwon, and Hyoung-Gon Kim. “Smart Location Tracking System using FSR (Force Sensing Resistor)”. In: *ICAT* ().
- [37] Somer M.Nacy, Mauwafak A.Tawfik, and Ihsan A.Baquer. “Static and Dynamic Calibration for Flexiforce Sensor Using a Special Purpuse Apparatus”. In: *ISSN 4.1* (2013), pp. 30–40.
- [38] Andrew clark, sunita P.Ho, and Martine LaBerge. “Conductive composite of UHMWPE and CB as a dynamic contact analysis sensor”. In: *Tribology International* 39 (2006).
- [39] Andrew clark. *Sensor Film Kits*. URL: [Link](#).
- [40] *Technical Product Data Sheets*. Plastic product Inc. URL: [Link](#).
- [41] Andrew clark. *SmartMat: Wi-Fi floor mat that can alert mobile devices*. URL: [Link](#).
- [42] *Arduino UNO overview available at <https://www.farnell.com/datasheets/1682209.pdf>*.
- [43] *USER GUIDE NI USB-6001/6002/6003 Low-Cost DAQ USB Device*.
- [44] *Atmel 8-bit AVR Microcontroller-ATmega328-328P*.
- [45] *The UHMWPE Handbook: Ultra-High Molecular Weight Polyethylene in Total Joint Replacement*. Technology and engineering, 2004.

# Appendix A

## Appendix A

Newton-Raphson Method (Multi-Variate)

The above method can be generalized to multi-variate case to solve n simultaneous algebraic equations

$$f_1(x_1, \dots, x_n) = f_1(x) = 0, f_n(x_1, \dots, x_n) = f_n(x) = 0 \quad (\text{A.1})$$

where  $\mathbf{x} = [x_1, \dots, x_n]^T$  is an n-dimensional vector. This equation system can be more concisely represented in vector form as  $\mathbf{f}(\mathbf{x}) = 0$ . The Newton-Raphson formula for multi-variate problem is

$$\mathbf{x} \leftarrow \mathbf{x} - J_f^{-1}(\mathbf{x})\mathbf{f}(\mathbf{x}) \quad (\text{A.2})$$

where  $J_f(\mathbf{x})$  is the Jacobian of function  $\mathbf{f}(\mathbf{x})$ :

$$J_f(\mathbf{x}) = \begin{bmatrix} \frac{\partial f_1}{\partial x_1} & \dots & \frac{\partial f_1}{\partial x_n} \\ \dots & \dots & \dots \\ \frac{\partial f_n}{\partial x_1} & \dots & \frac{\partial f_n}{\partial x_n} \end{bmatrix}$$

To derive this iteration, consider Taylor series

$$f_i(\mathbf{x} + \delta\mathbf{x}) = f_i(\mathbf{x}) + \sum_j \frac{\partial f_i}{\partial x_j} \delta x_j + O(\delta\mathbf{x}^2) \quad (i = 1, \dots, n)$$

We ignore the terms of  $\delta\mathbf{x}^2$  and higher and let  $f_i(\mathbf{x} + \delta\mathbf{x})$  be zero (i.e.,  $\mathbf{x} + \delta\mathbf{x}$  is the zero-crossing of the tangent), and get

$$\sum_j \frac{\partial f_i}{\partial x_j} \delta x_j = -f_i(\mathbf{x}) \quad (i = 1, \dots, n)$$

Solving this linear equation system for  $\delta x_j$ , we get

$$\delta\mathbf{x} = -J_f^{-1}(\mathbf{x})\mathbf{f}(\mathbf{x})$$

and the Newton-Raphson formula:

$$\mathbf{x} \leftarrow \mathbf{x} + \delta\mathbf{x} = \mathbf{x} - J_f^{-1}(\mathbf{x})\mathbf{f}(\mathbf{x})$$

# Appendix B

## Appendix B

- *Impact strength*: In materials science, the strength of a material is its ability to withstand an applied load without failure or plastic deformation.
  
- *Yield strength*: is the lowest stress that produces a permanent deformation in a material.
  
- Young's modulus :measures the resistance of a material to elastic (recoverable) deformation under load.  
A stiff material has a high Young's modulus and changes its shape only slightly under elastic loads (e.g. diamond). A flexible material has a low Young's modulus and changes its shape considerably (e.g. rubbers).

### **ABOUT UHMWPE:**

The Ultra High Molecular Weight Polyethylene is a subset of the thermoplastic polyethylene. It is characterized by extremely long chains, with a molecular mass usually between 3.5 and 7.5 million amu. The longer chain serves to transfer load more effectively to the polymer backbone by strengthening inter-molecular interactions. This results in a very tough material, with the highest impact strength of any thermoplastic presently made. [45] UHMWPE has also the highest abrasion resistance of any plastic. The following table presented by **Plastic Product Inc** presents some typical values of a 1" slab.

<b>Physical Properties</b>	<b>ASTM Test Method</b>	<b>Units</b>	<b>UHMWPE</b>
Density	D792	gm/cm <sup>3</sup>	0.926 - 0.934
Water absorption,	D570	%	Nil
<b>Mechanical Properties</b>	<b>ASTM Test Method</b>	<b>Units</b>	<b>UHMWPE</b>
Tensile Strength at yield	D638	MPa (ksi)	21 (3.1)
Tensile Strength at break	D638	MPa (ksi)	48 (7.9)
Elongation at break	D638	%	350
Young's Modulus			
At 23°C (73°F)	D638	GPa (10 <sup>6</sup> psi)	0.69 (0.10)
At -40°C (-40°F)	D638	GPa (10 <sup>6</sup> psi)	0.69 (0.10)

Figure B.1: Mechanical properties of UHMWPE

# Appendix C

## AppendixC

- *Circumduction:* is a conical movement of a limb extending from the joint (e.g. shoulder or hip) at which the movement is controlled. True circumduction allows for 360 degrees of movement.
- *dorsiflexion:* The movement which decreases the angle between the sole of the foot and the back of the leg.
- *steppage gait:* It is a form of gait abnormality which is characterized by foot drop due to loss of dorsiflexion.  
The foot hangs with the toes pointing down, causing the toes to scrape the ground while walking, requiring someone to lift their leg higher than normal when walking
- *Hip hiking:* a hip instability that comes from an abnormal hip alignment, such as a lateral pelvic twist or lift
- *hyperextension:* is a common injury among athletes, soccer players mostly. It happens when the knee is forced to extend more than regular.

# Appendix D

## Appendix D

### Component specification

#### D.1 NI-USB 6002

##### Analog Input

---

Number of channels	
Differential.....	4
Single-ended.....	8
ADC resolution.....	16-bit
Maximum sample rate (aggregate).....	50 kS/s
Converter type.....	Successive approximation
AI FIFO.....	2,047 samples
Trigger sources.....	Software, PFI 0, PFI 1
Input range.....	±10 V
Working voltage.....	±10 V
Input impedance.....	>1 GΩ
Input bias current.....	±200 pA
Absolute accuracy	
Typical at full scale.....	6 mV
Maximum over temperature.....	26 mV

## Analog Output

---

Analog outputs .....	2
DAC resolution .....	16-bit
Output range .....	$\pm 10$ V
Maximum update rate .....	5 kS/s simultaneous per channel, hardware-timed
AO FIFO .....	2,047 samples
Trigger sources .....	Software, PFI 0, PFI 1
Output current drive .....	$\pm 5$ mA
Short circuit current .....	$\pm 11$ mA
Slew rate .....	3 V/ $\mu$ s
Output impedance .....	0.2 $\Omega$

## Timebase

---



**Note** The following specifications apply to the sampling accuracy for hardware-timed analog input and analog output.

Timebase frequency .....	80 MHz
Timebase accuracy .....	$\pm 100$ ppm
Timing resolution .....	12.5 ns

## Digital I/O

---

### 13 digital lines

Port 0 .....	8 lines
Port 1 .....	4 lines
Port 2 .....	1 lines

### Function

P0.<0..7> .....	Static digital input/output
P1.0 .....	Static digital input/output
P1.1/PFI 1 .....	Static digital input/output, counter source or digital trigger
P1.<2..3> .....	Static digital input/output
P2.0/PFI 0 .....	Static digital input/output, counter source or digital trigger



## D.2 Arduino Uno

### ARDUINO UNO Revision 3 Specifications



- Microcontroller: ATmega328
- Operating Voltage: 5V
- Uno Board Recommended Input Voltage: 7 – 12 V
- Uno Board Input Voltage Limits: 6 – 20 V
- Digital I/O Pins: 14 total – 6 of which can be PWM
- Analog Input Pins: 6
- Maximum DC Current per I/O pin at 5VDC: 40ma
- Maximum DC Current per I/I pinat 3.3 VDC: 50ma
- Flash Memory: 32KB (0.5KB used by bootloader)
- SRAM Memory: 2KB
- EEPROM: 1KB
- Clock Speed: 16 MHz

### ARDUINO UNO Revision 3 Processor Peripherals (Atmel ATmega 328)

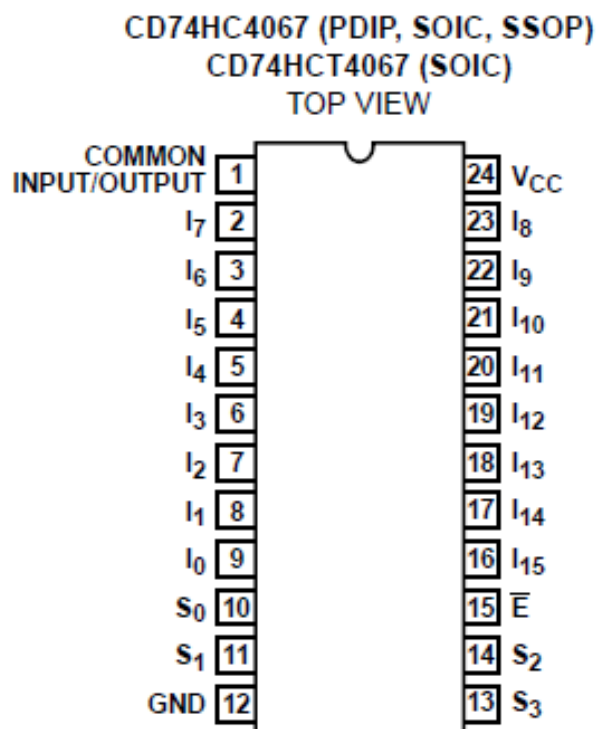


- Two 8-bit Timer/Counters with Separate Prescaler and Compare Mode
- One 16-bit Timer/Counter with Separate Prescaler, Compare Mode, and Capture Mode
- Real Time Counter with Separate Oscillator
- Six PWM channels
- Six channel 10 bit ADC including temperature measurement
- Programmable Serial USART
- Master/Slave SPI Serial Interface
- Byte-oriented 2 wire Serial Interface (Philips I2C compatible)
- Programmable Watchdog Timer with Separate On-chip Oscillator
- On-chip Analog Comparator

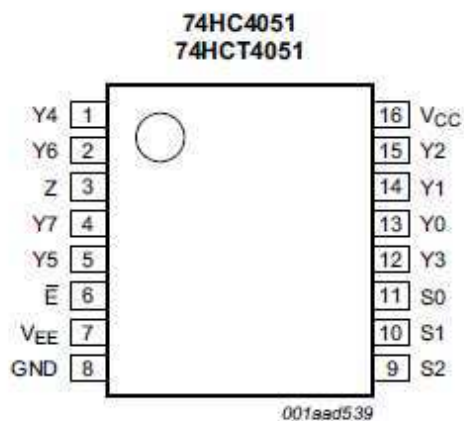
# PIN configuration

## D.3 Multiplexer

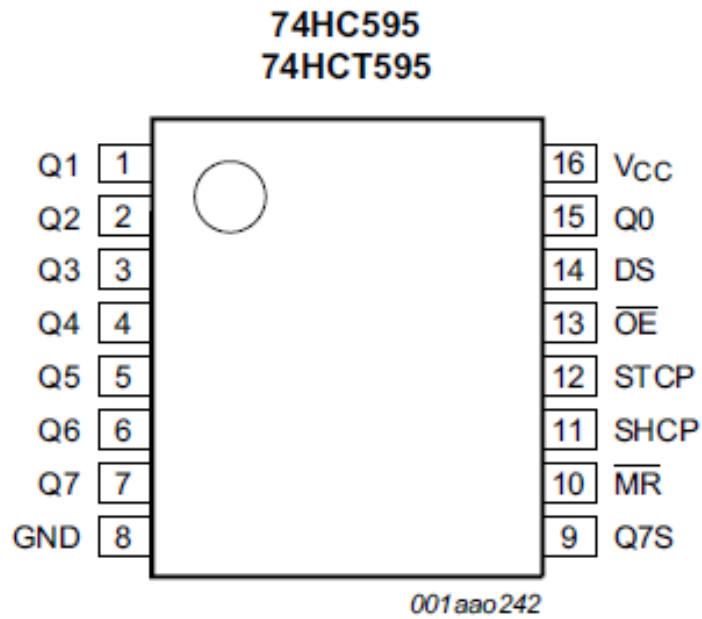
### Mux/Demux 16 to 1 -74HC4067



### Mux/Demux 8 to 1 -74HC4051



## D.4 Shift Register



## D.5 Operational Amplifier LM324

